JPRS-UMS-92-015
16 October 1992

FOREIGN
BROADCAST
INFORMATION
SERVICE

JPRS Report

Science & Technology

Central Eurasia: Materials Science

Science & Technology
Central Eurasia: Materials Science

JPRS-UMS-92-015

CONTENTS

16 October 1992

ANALYSIS, TESTING

COATINGS

COMPOSITE MATERIALS

FERROUS METALS

NONFERROUS METALS, ALLOYS, BRAZES, SOLDERS

NONMETALLIC MATERIALS

PREPARATIONS

TREATMENTS

WELDING, BRAZING, SOLDERING

EXTRACTIVE METALLURGY, MINING

MISCELLANEOUS

Structure of EK 62 Alloy After High-Temperature Plastometric Tests

927D0218E Dnepropetrovsk METALLURGICHESKAYA I GORNORUDNAYA PROMYSHLENNOST: NAUCHNO-TEKHNICHESKIY I PROIZVODSTVENNYY SBORNIK in Russian No 2, Apr-Jun 92 pp 35-36

[Article by V. Ye. Pilguk, V. V. Burkhovetskiy, M. P. Gazhura, Donetsk Scientific Research Institute of Ferrous Metallurgy; UDC 620.186.4-977:669.14-416]

[Abstract] To manufacture sheet and foil from the new high-temperature alloy EK 62, it was necessary to determine this alloy's plastometric characteristics in the proposed range of rolling rates and temperatures. Scanning electron microscopy and micro x-ray spectral analysis were used to investigate the alloy's structure after plastometric tests in a temperature range of 850-1200 degrees C. It was found that in its initial state, the primary phases of cast EK 62 are a gamma-matrix and a gamma'-phase of the Ni_3Al type which contain nickel, iron, chromium, molybdenum, niobium, titanium and carbides. For the matrix, chemical inhomogeneity for such elements as molybdenum, niobium, iron, nickel and chromium is characteristic. As the heating temperature rises, the chemical inhomogeneity decreases. With heating to 1000 degrees C, formation of an acicular phase is observed having a higher content of chromium and iron, and a lower content of niobium and molybdenum in comparison with the gamma'-phase. For the structure of the alloy tested at 1000 degrees C, it was characteristic that microcracks formed along clusters of electron compounds and carbides.

Evaluation of the Life of an Offshore Stationary Platform

927D0160D Kiev TEKHNICHESKAYA DIAGNOSTIKA I NERAZRUSHAYUSHCHIY KONTROL in Russian No 1, Jan-Feb-Mar 92 pp 44-51

[Article by E. F. Garf, A. Ye. Litvinenko, M. A. Mikitarenko, Z. M. Tairli, and A. F. Ismailov, Paton Institute of Electrical Welding, Ukrainian Academy of Sciences, Kiev, Ukrainian Scientific Research and Design Institute for Steel Structurals, Kiev, and State Scientific Research and Planning Institute of Offshore Oil and Gas Drilling, Baku; UDC 620.19.669.15.194.3]

[Abstract] The service life of the supporting structure of an offshore stationary drilling platform for the Caspian Sea was calculated. Calculation was based on data on wave activity in the region of installation, dynamic calculation of the structure, and calculation of the fatigue strength of tubular weldments used in the structure. The study focused on tubular weldments as the weakest elements in the structure. Dynamic calculations were made of the structure under the action of wave loads, and time variables of these loads as well as time variables of components of internal forces in critical structural elements were established. Analysis of the level of internal forces for elements of the four most heavily loaded weldments showed that the greatest forces take place in weldment No. 129, whose durability determines the life of the whole structure. From dynamic calculations, maximum scales of forces in elements of this weldment were determined for each level of wave activity. A procedure was followed which examined each element successively and established scales of forces for it for all levels of wave activity. A table is given showing the scales for three levels of wave activity with the time variables of waves. The scales of internal forces served as a basis for establishing scales of stresses in welds along directions of chords and braces. A calculation curve for fatigue of tubular weldments was used to determine the number of stress cycles at given scales of stresses, and a fatigue limit for weldments in the marine environment was calculated. A table is given with data necessary for determining the accumulated fatigue damage in one year of operation of the platform. Using a hypothesis of linear accumulation of fatigue damage and factoring in a deduction for the effect of the marine environment and a safety factor for fatigue cracking in one critical weld location, the period of safe operation of the platform is reckoned to be 6.25 years. This period is said to be significantly shorter than the planned period of operation of the platform.

Computer-Aided Diagnostics of Surface-Hardened Layers of Ferromagnetic Materials. 1. Layer Analysis of Stresses in Surface Layers Using the Barkhausen Effect

927D0160B Kiev TEKHNICHESKAYA DIAGNOSTIKA I NERAZRUSHAYUSHCHIY KONTROL in Russian No 1, Jan-Feb-Mar 92 pp 32-38

[Article by V. L. Vengrinovich, M. A. Knyazev, and A. L. Vishnevskiy, Institute of Applied Physics, Belorussian SSR Academy of Sciences, Minsk; UDC 620.179.14]

[Abstract] Principles of layer analysis of surface-hardened layers of ferromagnetic steels and cast irons using the Barkhausen effect are discussed, and a computer complex for applying the discussed approach is described. The approach makes it possible to obtain quantitative results. It is based on three main considerations: 1) energy parameters of noises from the Barkhausen effect have a high magnetoelastic sensitivity ; 2) stochastic electromagnetic damping caused by Barkhausen abrupt changes has unique characteristics; 3) mathematical methods of restitution of functions according to results of indirect measurements are widely used for applied tasks, particularly in tomography. Taken as essential a priori information for the approach is the dependence of the transducer's signal on the current variable at different stresses given the condition that in each experiment, the stress value does not change along a coordinate measured from the surface down into a space with semi-infinite dimensions. The approach depends on a set of basic a priori information. In preparing this information, a specimen in the form of a plate is bent, and a stress value is established for every deflection based on measurements and solution of a differential equation. The method of gathering basic a priori information, which is essentially a two-dimensional calibration dependence, consists in finding two coefficients of an exponential polynomial which approximates this dependence. This is accomplished by successive bending of a reference specimen with different degrees of deflection (compressive and tensile) at different amplitudes of reverse-magnetization current, and obtaining discrete values for stresses and currents and approximating the calibration dependence by the method of least squares. The coefficients thus obtained are entered into a computer and become specific for given brands of steel, and they are used

as basic a priori information in obtaining curves for specific products. This linear approximation model for stresses is used in the TOMOSKOP computer complex, which is intended for monitoring stressed states in surface layers of structural ferromagnetic materials. The components of the TOMOSKOP as well as its operating principle and software are described, and two figures are given showing stress curves in the surface layer of one brand of steel which were plotted by the TOMOSKOP.

Acoustic Emission Sensitization Transducers for Flexible Production Modules

927D0160E Kiev TEKHNICHESKAYA DIAGNOSTIKA I NERAZRUSHAYUSHCHIY KONTROL in Russian No 1, Jan-Feb-Mar 92 pp 52-57

[Article by V. Ye. Vaynberg, Kishinev Agricultural Institute; UDC 621.791.052.08:620.170.16]

[Abstract] Two acoustic emission transducers which were developed for automated control of machine tools in flexible production modules are described. The first transducer is an AE contact transducer for determining the positioning of cutting tools and/or workpieces in numerically controlled machine tools. The transducer is mounted in the spindle or some other part of the machine, and the coordinates of the tip of its probe are entered into the memory of the machine's program control unit. The probe comes into contact with the edge of the cutting tool or the reference plane of the workpiece. As it operates the coordinates of the probe's tip are continuously determined by the machine's coordinate system and entered into its control unit, and at the moment of contact the coordinates of the probe's tip corresponding to coordinates of the tool's cutting edge or the plane of the workpiece are recorded. The contact transducer contains a piezoelectric element which is attached to a metallic protective membrane, and an elastic probe is attached at an angle of 45 degrees to the membrane, which allows bending of the probe to move it to the monitored surface from any direction. A diagram of the contact transducer is given, as well as a flow chart of the mechanism which generates the contact signal. This mechanism consists of contact transducers connected in sequence, an amplifier with a set of filters for eliminating acoustical and electrical noise, a pulse shaper, and a shaper for pulses with a duration of 1 microsecond from the leading edge of the first AE pulse. The operation of the signal-generating mechanism is described. It is said that in tests of the contact transducer, the AE signal was generated upon movement of the transducer of not more than 1 micrometer after its contact with the supporting plane. The second transducer is a surface roughness measurement transducer. Research showed that the acoustic emission method is able to provide reliable information on the roughness of a machined surface, even in automated machining. The transducer developed for this operates on the principle that when two solids rub against each other, there occur microfractures which give rise to AE signals, the parameters of which depend on the condition of the rubbing surfaces. The roughness measurement transducer has a piezoelectric element attached to a metallic protective membrane, to which an elastic probe is welded. The probe's tip is made in diameters smaller than the average spacing of surface roughnesses for different degrees of surface finishes on which the transducer is used, so that the probe can fit into valleys between roughnesses. The trajectory of the probe's movement is thus affected by both the spacing, which changes the intensity of AE signals, and the height of roughnesses, which changes the amplitude of signals. The operation of the transducer and the measurement unit is explained; a diagram of the transducer and a flow chart of the measurement unit are given. In use, an operator sets the time of exposure with the transducer using a control signal generator, and the transducer records the amplitude, rate of counting, and the total number of AE signals. The set-up of a test of the roughness measurement transducer and its results are described. It is said that the recorded AE amplitudes qualify the transducer for use in monitoring the finish of surfaces machined down to Rz = 0.8 micrometers. It offers the advantage of monitoring the quality of machining with automated machine tool modules immediately upon completion of the machining cycle.

Investigation of the Electrification of Polymers During Friction in Vacuum

927D0194E Minsk TRENIYE I IZNOS in Russian Vol 13, No 3, May-Jun 92 pp 473-478

[Article by S. I. Guzenkov and A. F. Klimovich, Institute of the Mechanics of Metal-Polymer Systems of the Belarus Academy of Sciences, Gomel; UDC 541.6+537.212]

[Abstract] The electrification of high density polyethylene, polycaproamide, and polytetrafluorethylene during friction in vacuum was studied. The materials were first cleaned in a vacuum of 10^{-5} mm Hg at a temperature of 383 to 393 K for 4 h. Friction was created between the polymers and metals by setting them up as a shaft and partial bushing assembly in a specially made tester with an attachment to accomodate an Mkh-7301U42 mass spectrometer. The degree of electrification was estimated from the values for the frictional electricity current, which was recorded with the aid of self-adjusting P-325 microvoltnanoamperometer. The spectrometer was used to qualitatively analyze the volatile products released during the friction process. The results showed that frictional electrification is more intense in vacuum than at atmospheric pressures. Increasing the load leads to an increase in the values for the triboelectrification current and to a decrease in the time that elapses between the moment when friction begins and the onset of the first inversion in the current. The kinetics of the electrification current are similar at both vacuum and atmospheric pressures. It was shown that the first inversion of electrification current is caused by the desorption of water from the surface layers of the polymers. Figures 5; references 9: 7 Russian, 2 Western.

X-Ray Diffraction Analysis of Fe-Al-C Melts

927D0206E Kiev METALLOFIZIKA in Russian Vol 14 No 2, Feb 92 (manuscript received 11 Sep 91) pp 46-52

[Article by L.Ye. Mikhaylova, T.M. Khristenko, A.V. Romanova, V.A. Andryushchenko, and Ye.I. Nikolaychuk, Institute of Metal Physics at Ukrainian Academy of Sciences, Kiev; UDC 532.74:539.26:669.15-196]

[Abstract] Melts of three Fe-Al alloys with a 25 wt.% (10 atom.%) carbon content each and 4.0 wt.% (7.30 atom.%) Al, 7.0 wt.% (12.42 atom.%) Al, 11.0 wt.% (18.83 atom.%) Al respectively were examined by the x-ray diffraction method prior to their crystallization, the purpose being to establish

the influence of their liquid state condition on their structurization in the solid state and particularly on formation of binary iron-aluminum carbide (K-phase). In the solid state, after having been water-quenched from 1200°C to room temperature, these three alloys contained 50 % austenite + 50 % α-martensite, 45 % austenite + 25 % α-martensite + 30 % binary iron-aluminum carbide, 5 % austenite + 5 % α-martensite + 10 % aluminum ferrite + 80 % binary iron-aluminum carbide respectively. When already solid, the alloys were analyzed in a DRON-3 x-ray diffractometer, which yielded sufficient data for calculating the degree of long-range atomic order in K-phase particles in the two alloys containing it (0.65 and 0.92 respectively). When still in the liquid state, the alloys were analyzed in a high-temperature θ-θ x-ray diffractometer with the MoK_{α}-radiation source rotating about a horizontal axis and with a graphite monochromator for the primary x-ray beam. On the basis of the readings were then calculated the two structural factors: i(s) (s- diffraction vector) and radial atom distribution function. The model of these alloy melts which fits the experimental data best is one in which two kinds of atomic microclusters are forming: 1) clusters containing only Fe and probably C atoms with a b.c.c. structure of the short-range order, 2) clusters containing Al atoms, also some Fe and C atoms, with a close-packed K-phase structure. This model is consistent with the experimentally established evidence that neither the most likely interatomic distance, determined by location of the first maximum of the radial atom distribution function, nor the area under the first peak of this function change as the aluminum content increases. Figures 2; tables 2; references 25.

Magnetic Properties and Structural Transformations of Amorphous Microconductor During Heating

927D0206F Kiev METALLOFIZIKA in Russian
Vol 14 No 2, Feb 92 (manuscript received 17 Jul 91; final version received 9 Jan 92) pp 53-57

[Article by Ye.N. Khandogina, A.L. Petelin, Yu.A. Birman, and N.P. Vasilyeva, Central Design Office for Special Radio Engineering Materials, Moscow; UDC 548.4+539.3]

[Abstract] An experimental study of three amorphous microconductor materials $(Fe,Co,Ni)_{75}B_{15}Si_{10}$ was made concerning the never before determined temperature dependence of their structure and magnetic properties, a microconductor of any amorphous material being produced by extrusion of a glass capillary containing the molten material and simultaneously quenching it. Strands of the Fe-B-Si alloy 8-15 μm in diameter and strands of the Co-B-Si alloy 10-18 μm were combined into 35 mm long cylindrical microconductors 2-3 mm in diameter for measurement of their magnetization in an anisometer while they were being heated over the 0-800°C range in the continuous mode at a rate of 20 K/min, the instrument having an induction sensitivity of 20 G and an error not larger than 1 % of maximum magnetization. Then, after having been annealed at various temperatures covering the 300-700°C range, they were subjected to x-ray structural and electron microscope examination. The structure of the metal-glass transition interlayer was examined in a Stereoscan x-ray microspectroscope with a Link energy dissipating attachment. Microconductors with Fe-B-Si strands were also tested for the effect of glass insulation and attendant tensile stresses on their magnetic properties. These tests were performed in a vibromagnetometer in three ways: 1) by plotting the hysteresis loops of one microconductor along and across its axis; 2) by plotting the hysteresis loops of several microconductors having all the same overall diameter but each containing strands of a different size; 3) by plotting the magnetization curve and measuring the dynamic a.c. characteristics of microconductors wound on two toroidal cores 13 mm and 2.5 mm in diameter respectively, with magnetizing currents of several different frequencies from 1 kHz (on 13 mm core) or 10 kHz (on 2.5 mm core) to 200 kHz. Microconductors with Ni-B-Si strands were examined for the distribution of metal (nickel) and silicate glass in the transition interlayer at temperatures covering the 650-500°C crystallization range, the Ni content found to be increasing with higher annealing temperature. Figures 4; references 3.

Optical Properties of Multilayer Tb-Fe Film Structures

927D0206C Kiev METALLOFIZIKA in Russian
Vol 14 No 2, Feb 92 (manuscript received 3 Sep 91) pp 27-31

[Article by O.Yu. Bzhestovskiy, Yu.V. Kudryavtsev, and S.Ya. Kharitonskiy, Institute of Metal Physics at Ukrainian Academy of Sciences, Kiev; UDC 535.331:669.01]

[Abstract] An experimental study of thin multilayer Tb_xFe_{1-x} films with layers of nanometric thickness was made, multilayer films but only thin ones having been found to perform better than homogeneous ones as magnetooptical recording and data storage media. An explanation for this is sought in the role of interlayer boundaries, and confirmation is found in the analysis of optical conductivity spectra. Four batches of 100-120 nm thick films with respectively 10 nm, 6 nm, 3 nm, 0.5 nm thick Tb and Fe layers were produced by alternating the deposition of Tb and Fe from a separate electron-arc source but at the same rate of about 1.5 nm/s each, under a vacuum of about 5 mPa on fused-quartz substrates at a 293 K temperature. The principal object of this study were films with x = 22-24 atom.% Tb, but simple $Tb_{24}Fe_{76}$ films as well as pure Tb and Fe films were also produced and tested under analogous conditions. The free surface of each film was protected by an Al_2O_3 coating against oxidation. Their refractive index n and absorption coefficient k, for light of various wavelengths covering the 480-690 nm (3.5-1.5 eV) region of the spectrum, were measured from the substrate side by the Beattie method at a 293 K temperature and with a 73° angle of incidence. The substrates were Dove prisms with the two lateral faces inclined each at a 73° angle to the base so that reflection by those faces did not introduce additional polarization. The optical conductivity was then calculated and its frequency (energy) dependence evaluated according to the relation $\sigma(\omega) = nk\omega/2\pi$. The distribution of Tb and Fe in the layers was determined by way of Auger electron spectroscopy with ionic surface etching. The test data on films with 10 nm layers fit the model of a multilayer Tb-Fe film as a stack consisting of a 7 nm thick Fe layer followed by so many alternating 10 nm thick (6 nm Tb-Fe / 4 nm Tb) and (6 nm Tb-Fe / 4 nm Fe) layers until a total film thickness of 120 nm is approached and reflection of light by the substrate becomes correspondingly negligible. The optical properties of the Tb-Fe transition interlayers between high-Tb and high-Fe layers in such a stack are evidently identical to those

of 6 nm thick simple Tb-Fe films. The test data on films with 6 nm thick layers do not fit an analogous model, evidently because the thickness of the Tb-Fe transition interlayers exceeds 1.5 nm. The principal mechanism by which the Tb-Fe transition interlayers acquire their optical properties is revealed by the test data on simple $Tb_{24}Fe_{76}$ films. These films were originally amorphous, but became crystalline upon being heated to about 500 K at a rate of 3 K/min. Crystallization changed temperature dependence of their electrical resistance and the form of their optical conductivity spectrum, each now closely resembling the respective characteristic of the Tb-Fe transition interlayers in multilayer Tb-Fe films. One therefore may conclude that the material of those transition interlayers is crystallized $Tb_{24}Fe_{76}$ alloy. Figures 5; references 9.

Electronic Structure and Desorption Processes in $TiCoH_x$ Hydrides

927D0206B Kiev METALLOFIZIKA in Russian Vol 14 No 2, Feb 92 (manuscript received 2 Jul 91; final version received 6 Nov 91) pp 18-25

[Article by V.V. Nemoshkalenko, Ye.V. Sedyakina, V.A. Yatsenko, N.S. Kobzenko, and L.M. Sheludchenko, Institute of Metal Physics at Ukrainian Academy of Sciences, Kiev; UDC 537.531:3]

[Abstract] An experimental study of one β_1-phase TiCo hydride ($TiCoH_{0.88}$) and two β_2-phase TiCo hydrides ($TiCoH_{1.42}$, $TiCoH_{1.5}$) was made concerning their electronic structure and thermal stability, all three having orthorhombic lattices with different parameters each. Stoichiometric TiCo was produced by fusion of extra-pure titanium and cobalt iodides in an electric-arc furnace with a nonconsumable electrode, the ingots of this intermetallic compound being homogenized at 1100°C for 24 h and then cut into 2 mm thick slices with an ordered b.c.c. lattice structure. After the oxide surface film had been removed, the slices were ground to powder in a steel mortar at a liquid-nitrogen temperature. The powder was stress-relieved by annealing in a cup made of molybdenum foil and sealed inside a quartz flask under a vacuum of 1.3 Pa, the flask also containing TiI_2 chips as a getter substance. Following a sieve analysis, TiCo powder of the 1-1.6 mm grains size fraction was hydrogenated at various temperatures covering the 273-723 K range, under various pressures covering the 2-10 MPa range. This was done in the IVGM-2M apparatus specially built at the Institute of Metal Physics for such operations. The hydrogen content in each hydride was monitored independently by gravimetric analysis and by gas analysis with an evalograph using a hydrogen detector. The electronic structure of the three hydride powders was determined on the basis of x-ray emission spectroscopy. The K-emission spectra of titanium and cobalt were obtained with an DRS-2M long-wave x-ray spectrograph, atoms of both metals being excited by a BKhV-7 fluorescent x-ray tube with copper and chromium anodes. The $L\alpha_{1,2}$-emission spectra of titanium were obtained with an RSM-500 ultralong-wave spectrometer-monochromator set using electronic excitation, the x-ray tube operating in the 3 kV 1-2 mA mode. The L-emission spectra of cobalt were obtained with a SARF-1 fluorescent long-wave spectrometer using an RbAP crystal as analyzer, the x-ray tube with a copper anode operating in the 6 kV 600 mA mode. The thermal stability of the three hydrides was determined on the basis of a correlation between the d-electron concentration in titanium at the Fermi level and the hydride decomposition temperature, this temperature having been determined from desorption data. Desorption was tracked in the heating mode, hydride specimens weighing 0.7 g being placed in alundum crucibles and there heated at a rate of 5 K/min by a helium stream flowing at a rate of 14 cm^3/sec. The data indicate that the region of the valence band near the Fermi level in all three hydrides is formed by electronic p-states and d-states of metal atoms, while the "hydrogenated" band containing hybridized electronic s-state of hydrogen atoms consists of two subbands with approximately -6 eV and -9 eV median levels respectively. Inasmuch as d-electrons of Co atoms do not appreciably participate in formation of the hydride band, they are chemically sluggish in forming Co-H bonds. A correlation between electronic structure and thermal stability does indeed exist, inasmuch as an increase of the concentration of valence electrons at the Fermi level has been found to lower the thermal stability of the hydrides. The authors thank V.N. Uvarov for discussing the results. Figures 5; references 22.

Mass Transfer in Mo and Mo:Re Crystals Under Impact Load

927D0206H Kiev METALLOFIZIKA in Russian Vol 14 No 2, Feb 92 (manuscript received 10 Jul 91; final version received 19 Dec 91) pp 96-100

[Article by M.N. Belyakova, V.V. Zholud, L.N. Larikov, and V.F. Mazanko, Institute of Metal Physics at Ukrainian Academy of Sciences, Kiev; UDC 539.379.3:669.017.3]

[Abstract] Anomalous mass transfer in metals under impact loads is analyzed on the basis of theory and experimental data, experiments having been performed with Mo and Mo + Re(10 atom.%,17 atom.%) single crystals (b.c.c. lattice) after three successive zone refining treatments. Cylindrical specimens of such crystals, 3 mm high and 10 mm in diameter, were electrolytically coated with an about 0.5 μm thick film of radioactive Ni-63 isotope. They were then compressed, at room temperature, along their 110-axis at strain rates of 200-300 sec^{-1} to not more than 19 % deformation. Under these conditions the strain distribution in pure Mo and in Mo + 10 atom.% Re crystals was found to have remained quite uniform over the entire mass transfer path, but in Mo + 17 atom.% Re crystals plastic deformation was found to have been enhanced by formation of microtwins. Mass transfer of the Ni-63 tracer during the deformation process was tracked by layerwise etching of the deformed specimens. Theoretical calculations are based on the approximate relation for the mean displacement of Ni-63 atoms under impact $\bar{x} = vt + 2(D^*t)^{1/2}$ (t- duration of impact pulse, v- drift velocity of atoms in field of glissile dislocations, D^*- diffusion coefficient), the effective diffusion coefficient being determined empirically by comparing the measured axial concentration profile with the ideal one in a semi-infinitely long body. The results of this study reveal that rhenium influences the migration of Ni-63 isotope through a molybdenum crystal by a combination of three mechanisms, each becoming more effective with increasing Re content: 1) it decreases the number of interstitial Mo atom and Ni-63 atom pairs, 2) it decreases the number of risers capable of gathering interstitial Mo atoms (increases the probability of such risers being split), 3) it

enhances the contribution of twinning to plastic deformation of the crystal. Figures 2; references 14.

Metastable Concentrational Inhomogeneities in Metallic Glasses

927D0206D Kiev METALLOFIZIKA in Russian Vol 14 No 2, Feb 92 (manuscript received 17 Jul 91) pp 38-45

[Article by V.P. Naberezhnykh, Donetsk Institute of Engineering Physics at Ukrainian Academy of Sciences; UDC 669.15'24:539.213:539.219.3]

[Abstract] Spinodal decomposition of solid solutions such as binary glassy alloys is analyzed theoretically on the basis of its geometrical description by a trajectory in the N-dimensional phase space which begins at the homogeneous unstable state and ends at the two-phase equilibrium, each intermediate concentration profile c(r) corresponding to a certain figurative point on this trajectory. The concentration profiles also satisfy the equation of one-dimensional motion of a classical nonlinear oscillator under an increasing force μ-dF(c)/dc, where the constant μ denotes the chemical potential and F(c) denotes the concentration-dependent free energy. Only energies V_{AA}, V_{BB}, and V_{AB} two-atom interactions are taken into account in the specific case of a disordered solid solution. On the basis of this model with the mixing energy $W = V_{AA} + V_{BB} - V_{AB}$ and absolute value of $W = 2kT_c$ has been evaluated the concentration dependence of the energy f'(c) = F(c)/absolute value of W = f(c) - μ/absolute value of Wc (both free energy and chemical potential normalized to absolute value of W) covering the entire c[0,1] concentration range at a temperature $T = 0.4T_c$ and a chemical potential $\mu = 0.15$ absolute value of W. There also have been established one lower and two alternative upper boundaries of the regions of existence of metastable steady states in both f'-c and T_r-μ' planes ($T_r = T/T_c$, $\mu' = \mu$/absolute value of W), specifically for solid solution with a $\bar{c} = 0.3$ mean concentration. The upper boundary is determined by two factors: 1) the f'(c) energy maximum, which does not depend on the mean concentration $\bar{c}$, must vanish; 2) the mean concentration cannot exceed the concentration which corresponds to maximum energy. Both minimum and maximum concentrations during decomposition depend on the temperature and on the chemical potential. As a special case is considered hardening of a solid solution into the metastability range and holding it at a constant temperature for a sufficiently long time it is further heated into successive new steady states and then cooled. The trends in such a treatment reveal a reversible and an almost if not exactly periodic oscillatory temperature dependence of the chemical potential and of the alloy composition, which explains low-angle scattering of x-rays as well as reversible relaxation of elastic stresses and electrical resistance in amorphous glassy alloys. Deformation of the concentration profile in such alloys into a nonuniform one by diffusion resulting in formation of inhomogeneities explains, moreover, the low-temperature creep similar to Herring-Nabarro creep in polycrystals. Figures 5; references 14.

Structural State and Phase Composition of Electroerosive Iron Powders Produced in Water

927D0206A Kiev METALLOFIZIKA in Russian Vol 14 No 2, Feb 92 (manuscript received 28 Nov 91) pp 14-17

[Article by K.V. Chuistov, A.Ye. Perekos, N.A. Tomashevskiy (deceased), O.I. Nosovskiy, V.P. Zalutskiy, T.V. Yefimova, and V.V. Polotnyuk, Institute of Metal Physics at Ukrainian Academy of Sciences, Kiev; UDC 621.762]

[Abstract] An experimental study of highly disperse iron powders produced by the electron discharge process in water was made, its purpose being to determine their structural state and phase composition along with their magnetic properties not only in the fresh state but also after lengthy soaking in water or aging in air. Two kinds of powder were produced under different conditions of dispersing treatment: one with a low oxide content (about 40 %) and one with a high oxide content (close to 100 %). Their phase composition was determined by three methods: 1) Mossbauer spectroscopy with an NGR nuclear-gamma-resonance spectrometer under constant acceleration in both transmission and reflection modes, geometries, using cobalt-57 embedded in chromium as source of resonance radiation; 2) x-ray structural analysis in a DRON-2.0 diffractometer with a FeK_α-radiation source; 3) thermomagnetic analysis with a ballistic magnetometer in magnetic fields of up to 800 kA/m, measuring the saturation magnetization at temperatures from room temperature to 600°C and higher. Their chemical composition was determined by means of Auger electron spectroscopy with a JAMP-10 spectrometer and a 25 nm in diameter electron probe, under a 10 kV accelerating voltage and a 0.5 μA current. The low-oxide powder was found to contain α-Fe (sextet in Mossbauer spectrum) and Fe_xO_{1-x} (two doublets in Mossbauer spectrum), most likely Fe_3O_4 (supermagnetic magnetite). One month long soaking in water, but not aging in normal air, changed both their structural state and phase composition. The high-oxide powder was found to contain both Fe_3O_4 and γ-Fe_2O_3 oxides. Two years long aging in normal air at room temperature, but not one month long soaking in water, changed both their structural state and phase composition. Chemical analysis revealed Fe and O atoms in all powder specimens, the concentrations of both elements in fresh specimens slightly fluctuating in time during the initial period and being almost uniformly distributed over the volume. The magnetization of high-oxide specimens containing magnetite decreased fast toward zero as the temperature was raised from 550°C to 600°C (Curie point), while the magnetization of high-oxide specimens not containing any magnetite (after aging in air) decreased fast toward zero within the 400-450°C range already. Figures 3; references 4.

Electron Diffraction Analysis of Interaction of Thin Ni and GaAs Films

927D0206G Kiev METALLOFIZIKA in Russian Vol 14 No 2, Feb 92 (manuscript received 15 Jan 91; final version received 23 Dec 91) pp 66-70

[Article by N.T. Gladkikh, I.P. Grebennik, S.V. Dukarov, M.S. Zoto, and I.V. Sorokina, Kharkov State University; UDC 539.216.2:621.315.592]

[Abstract] Interaction of Ni and GaAs layers in thin Ni/GaAs films was studied by the electron diffraction method, such films having been deposited on NaCl single crystals by vacuum evaporation and subsequent condensation under a residual pressure of 0.1 mPa. First were deposited the GaAs layers, by discrete evaporation on substrates so oriented relative to the evaporator as to ensure a uniform film thickness of about 30 nm. Then were deposited the Ni layers, by evaporation from a tungsten wire, their thickness

being varied over the 3-50 nm range. During condensation of GaAs, some substrates were at a 20°C temperature and some at a 400°C temperature. During subsequent condensation of Ni the temperature of all substrates was 400°C. Electron diffractometry of the films revealed eight phases: GaAs, NiAs, $NiGa_4$, Ni_2As_2, α-$NiAs_2$, Ni_3Ga_4, γ-Ni_3Ga_2, α'-phase. The phase composition of the films was found to depend on the film thickness, films with GaAs condensed at 20°C and films with GaAs condensed at 400° differing in structure as well as in the number and concentration of phases produced by Ni-GaAs interaction. Figures 2; tables 1; references 7.

Certain Features Unique to the Formation of Molybdenum-Nickel Coatings on Diamonds

927D0215D Kiev POROSHKOVAYA METALLURGIYA in Russian No 6, Jun 92 pp 23-28

[Article by V. G. Chuprina, I. M. Shalya, and V. V. Shurkhal, Institute of Problems in Materials Science of the Ukrainian Academy of Sciences; UDC 621.762: 621.793:669.24:669.28]

[Abstract] Change in the thickness and phase composition of molybdenum and nickel coatings on diamond powders was studied. Metallization was carried out at 750 and 950°C using metallizing mixtures with different oxygen concentrations. Metallization time varied from 0.25 to 4 hours. Coating thickness was measured by weighing the coated powders, which also underwent x-ray phase analysis. It was found that the coatings were formed largely as a result of reactions between the molybdenum oxides, which formed during the reduction of the nickel oxide by the molybdenum, and the carbon. In contrast to the metallization of diamond powders in an oxidized molybdenum powder, metallization in a mixture of NiO + Mo is characterized by the formation of a very thick coating, by the earlier formation of a solid coating, and a longer coating growth time, other conditions remaining the same. This is explained by the catalytic effect of the active (reduced) nickel on the reduction reaction and on carbide formation. Reactions between the reduced molybdenum and the active carbon, which forms during CO breakdown on the surface of the finely dispersed nickel, also contributes to the increase in coating mass. When, after 2 hours, the oxygen in the metallizing mixtures is depleted, this process becomes the primary one and is driven largely by the carbide composition of the external layers of the coatings. Figures 1, tables 2; references 13: 12 Russian, 1 Western.

Structure and Properties of Coatings Applied With a CO_2 Laser

927D0225D Moscow METALLOVEDENIYE I TERMICHESKAYA OBRABOTKA METALLOV in Russian No 7, Jul 92 pp 18-21

[Article by V. Ye. Arkhipov, A. A. Ablayev, and L. T. Krasnov, All-Union Scientific and Production Association "Remdetal"; UDC 621.9.048.7:621.762]

[Abstract] The structure and properties of 45 coatings applied to steel with a CO_2 laser were investigated. The coating materials used were self-fluxing nickel-base powders containing different amounts of carbide and boride forming elements. Different effects on the structure and properties of coatings were determined for different compositions of powder materials and different parameters of their application with the laser. Treated specimens were examined using the methods of metallographic analysis and luminescence analysis. The analyses produced the following conclusions:

1. Decreasing the chromium and carbon contents in the powder material of the system Ni-Cr-B-Si makes the coating less likely to crack.

2. Preheating the substrate specimen to 100-150 degrees C almost completely eliminates the tendency of the coating to crack when nickel-base self-fluxing powders are used as the coating material.

3. The corrosion resistance of coatings applied with the laser is as high as that of chrome-plating, and such coatings have a long service life even when cracks do form on the surface.

4. Coatings are highly resistant to scoring both at room temperature and higher temperatures, and their resistance to wear is an order of magnitude greater than the wear resistance of steel 45 which has been heat treated to a hardness of 51-53 HRC.

Roller Bearings With Solid Magnetic Powder Lubricant

927D0194A Minsk TRENIYE I IZNOS in Russian Vol 13, No 3, Oct 92 pp 460-464

[Article by Yu. N. Drozdov, R. I. Fishman, L. O. Weisfeld, and V. G. Pavlov, Institute of Machine Design imeni Academic A. A. Blagonravova of the USSR Academy of Sciences, Moscow; UDC 621.892]

[Abstract] Two types of rolling-contact bearings lubricated with magnetic powder were designed and tested. One of the bearings was a specially-designed thrust bearing with wire races. The other was a radial-thrust bearing of conventional construction. The bearings were designed so that the bearing components, along with additional magnetic components, work together to create within the bearing a non-uniform magnetic field capable of increasing in intensity as it approaches the working parts and friction zones of the bearings, thereby delivering lubricant from its repositories within the bearing structure to the friction zones. The thrust bearing was bench-tested using an electric motor and auxiliary equipment for regulating load, engine speed, temperature, pressure, and so forth. The tests were performed at atmospheric pressure and in vacuum. Bearing load was 1250 and 2500 N, engine speed was 10 and 50 c^{-1}, temperature was 20 and 300°C, and magnetic field strength in the gaps between the wire races was 25 and 40 kA/m. Three types of lubricant were used: a 3:1 mixture of graphite and cobalt, a 3:1 mixture of molybdenum disulfide and cobalt, and a mixture that was 93% C/Co lubricant and 7% teflon. After 1500 hours of testing, the bearing was completely functional and no sign of seizing or lubricant degradation was detected. Higher loads and magnetic field intensities induced higher friction moments; higher speeds induced lower friction moments. The friction moment curves had a shape that is usual for this type of friction system. The radial-thrust bearing, which was lubricated with a 30:70% mixture of gamma-iron oxide and molybdenum disulfide, was tested as part of a toothed reduction gear assembly in a 7×10^{-4}-Pa vacuum. Contact stress at the meshing point was 1000 MPa, sliding speed was 0.08 m/s, shaft revolution speed was 4.7 s^{-1}, and test temperature was 20°C. After 100 hours of testing, the bearing showed no signs of wear. Figures 3, tables 1, references 2: Russian.

Ceramic and Composite Materials and Their Properties

927D0213A Blagoveshchensk KERAMICHESKIYE I KOMPOZITSIONNYYE MATERIALY I IKH SVOYSTVA in Russian 89 pp 2-3, 143-144

[Annotation, Foreword, and Table of Contents of book by N. S. Kostyukov and Yu. T. Levitskiy "Ceramic Composite Materials and Their Properties," 1989, 144 pp

[Text]

Annotation

This anthology reviews problems in producing ceramic composite materials with special properties, the materials' properties and their change upon exposure to external forces, and certain problems in the procedure for studying the properties of ceramics and composite materials.

The anthology is intended for a broad audience of scientific, engineering, and technical personnel specializing in physics, chemistry, technology, and materials science. It will also be useful to teachers, graduate students, and undergraduate students in the corresponding fields.

Published by permission of the editorial department of the DVO AN SSSR [Far Eastern Division of the USSR Academy of Sciences].

Executive editor: N. S. Kostyukov, Yu. T. Levitskiy

Reviewers: P. P. Safronov, V. I. Poshin

Foreword

Under current conditions there is a particular need to expand efforts to create new technically valuable materials. A general trend in modern inorganic materials science is the production, study, and use of ceramic and composite materials of increasingly complicated composition.

In recent years ceramic and composite materials have been used in construction, electrical engineering, electronics, atomic power engineering, engineering physics, and special instrument building. Their introduction into nuclear power engineering, thermonuclear synthesis and other fields is imminent.

As efforts expand, ceramic and composite materials will exhibit new, original properties. The simple, cheaper, and more readily available the technology for manufacturing them, the more effective will advances in the use of these materials be.

This anthology includes works presented at the section on inorganic materials and ceramics at the Second Seminar School on Solid State Physics and Chemistry in 1988.

The anthology is devoted to the production of ceramic and composite materials with various compositions and the study of their properties.

By virtue of certain circumstances, the most attention has been given to ceramics among all inorganic materials. This has defined the basic contents of the anthology.

Ceramics are represented by a broad range of articles from problems of the systematics of ceramic materials to problems of resource-saving technologies for slag-containing materials.

Furthermore, the anthology contains works on procedural matters of conducting an experiment. A great deal of attention has been given to a discussion of the rational cost of the materials, which, just as metals, are highly radiation-proof and are being increasingly used in atomic and thermonuclear power engineering.

N. S. Kostyukov Yu. T. Levitskiy

Table of Contents

Development of Technology for Manufacturing High-Strength Pipe From Alloy 36NKhTYuM5

927D0218D Dnepropetrovsk METALLURGICHESKAYA I GORNORUDNAYA PROMYSHLENNOST: NAUCHNO-TEKHNICHESKIY I PROIZVODSTVENNY SBORNIK in Russian No 2, Apr-Jun 92 pp 19-20

[Article by A. V. Chub, I. P. Ostrovskiy, T. Ya. Vasilyeva, V. A. Omelchenko, All-Union Scientific Research Institute of Pipes; UDC 621.774:669.14.018.295]:621.78]

[Abstract] Research results are presented on the development of technology for manufacturing pipe from the alloy 36NKhTYuM5 with an ultimate breaking strength of at least 1400 H/mm^2 after age hardening. The basis selected for the technology was the deformation operations developed for the alloy 36NKhTYu, and heat treatment conditions (quenching and aging) were tailored specifically for alloy 36NKhTYuM5. It was shown that to achieve the necessary flattening of 3 and 4 mm in wall thickness and an ultimate breaking strength after age hardening of at least 1400 H/mm^2, quenching should be done with grain size no finer than No. 10 on the state standard scale GOST 5639-82, and aging should be at 750 degrees C for 4 hours.

New Designs of Continuous Casting Molds for Copper and Copper Alloys

927D0220I Moscow TSVETNYYE METALLY in Russian No 7, Jul 92 pp 56-58

[Article by V. A. Izmaylov, R. M. Fridlyanskiy, V. F. Goloveshko, and A. I. Suvorov, "Krasnyy vyborzhets" Production Association and State Research and Design Institute of Nonferrous Metal Alloys and Their Processing; UDC 669.35-147]

[Abstract] Several new designs of continuous casting molds tailored for different requirements of solidification of copper-based ingots are presented. The designs allow for different thermophysical properties and ingot sizes of cast copper alloys, including aluminum bronze and nickel silver. They provide for different schemes of water and steam-air cooling of ingots. All the designs have an improved cantilever mounting of the mold sleeve which makes it less likely to buckle in comparison with the rigid mountings of existing designs.

Development of an Efficient Process for Making Mg-Al-Zn-Mn Alloy Ingots in a Salt-Heated Furnace

927D0220H Moscow TSVETNYYE METALLY in Russian No 7, Jul 92 pp 39-42

[Article by V. I. Gribov, V. D. Yazev, V. A. Startsev, V. M. Agapov, Russian Titanium Institute and Solikamsk Magnesium Plant; UDC 669.721]

[Abstract] A salt-heated furnace developed for melting up to 35 tons per day of MA8Ts alloy at the Solikamsk Magnesium Plant is described. This furnace represents an improvement over an earlier design (1974-76) which was not very efficient and had excessive metal loss due to surface burn-up. In the new design, metal loss is reduced thanks to installation of a submersible bell which is constantly beneath the salt melt in a ring furnace. The design of the furnace and auxiliary equipment is described and process parameters are presented. Tables are given showing the composition of MA8Ts alloy and of secondary metal, the ratio of input and output materials in the process, and the furnace's energy balance. Two years of pilot-scale operation of the salt- heated furnace have shown the following results as compared with the earlier design: metal loss reduced by 20-25 kg/ton; power consumption reduced by 680 kW-hr/ton; reduced consumption of crucibles, Ni-Cr alloy and flux; and more efficient use of secondary alloy. The furnace and process have been awarded several patents, and have been recommended for full-scale industrial operation.

High-Temperature Oxidation of Nonmetallic Refractory Materials

927D0220G Moscow TSVETNYYE METALLY in Russian No 7, Jul 92 pp 33-35

[Article by Ye. S. Gorlanov, Yu. V. Borisogleskiy, M. M. Vetyukhov, S. N. Akhmedov, and L. N. Filatov, LGTU, All-Union Institute of Aluminum and Magnesium, OKT-BsOP IPM of Ukrainian Academy of Sciences; UDC 669.713.7:666.762.856]

[Abstract] To aid in the selection of refractory materials that can replace graphite for use in side linings of aluminum electrolyzers, oxidation kinetics of SiC, Si_3N_4, AlN, BN and their compositions in air in the temperature range 910-1060 degrees C were investigated. Oxidation kinetics curves for the materials were plotted using a method of continuous weighing developed at the All-Union Institute of Aluminum and Magnesium. A table of data is given for comparative analysis of the resistivity of the investigated materials to oxidation in air. The highest resistance to high-temperature oxidation in air was shown by a material consisting of 48.75% SiC, 48.75% Si_3N_4 and 2.5% MgO. This material has the drawback that there is some silicon contamination of the aluminum. AlN is another promising material that demonstrated high corrosion resistance. Compositions based on it (e.g., 70% AlN and 30% SiC) have much lower silicon activity in the material and consequently there is less silicon contamination of the aluminum. It was determined that conditions under which the refractory materials are sintered can have a big effect on their oxidation resistance, and therefore special studies of processes taking place in sintering of the materials should indicate ways of improving their performance characteristics for use in side linings of aluminum electrolyzers.

Processing of Flue Gas Into Sulfuric Acid Using Accelerated Electrons

927D0220F Moscow TSVETNYYE METALLY in Russian No 7, Jul 92 pp 24-27

[Article by V. D. Nagibin and S. L. Shevaleva, State Scientific Research Institute of Nonferrous Metallurgy; UDC 661.25]

[Abstract] The contact method for processing of flue gas into sulfuric acid which is currently used in nonferrous metals industry was borrowed from chemical industry and is suited to a rather narrow range (4-11%) of sulfur dioxide concentrations. In recent years the State Scientific Research Institute of Nonferrous Metallurgy has done research on the application of accelerated electrons in nonferrous metallurgy processes, including the treatment of gases containing sulfur with widely varying concentrations. The research indicated that under certain conditions, formation of sulfuric acid under the action of accelerated electrons in a gas-liquid medium (radiolysis) can proceed by a chain mechanism which permits the necessary degree of gas purification and can be realized in an efficient technological process. Theoretical calculations of the process are presented. The necessary conditions for it were determined to be: adequacy of the absorbed radiation dose for forming primary particles for radiolysis; presence in the gas flow of moisture in the form of aerosol particles in an amount close to stoichiometric for the formation of sulfuric acid; creation of liquid contacts between sulfur dioxide and nitrogen oxides; selection of a sprayable acid at a concentration and temperature having maximum solubility for sulfur dioxide. Laboratory studies using an electron accelerator confirmed theoretical calculations and led to construction of an experimental installation with a capacity of 20,000 cubic meters of flue gas per hour at the Novosibirsk Tin Combine. It uses an industrial ELV-4 electron accelerator with energy of 0.5-0.7 MeV and filament current up to 50 mA. In comparison with conventional technology, the advantages of the new process are: it does away with the need to build costly systems for catalytic oxidation of sulfur dioxide; it can

process gases with a wide range of sulfur dioxide concentrations; process control is simplified and it can be fully automated; it is more ecologically clean.

High-Temperature Sulfuric-Acid Leaching of Copper Matte in an Autoclave

927D0220E Moscow TSVETNYYE METALLY in Russian No 7, Jul 92 pp 23-24

[Article by S. S. Naboychenko and U. A. Ergashev, Urals Polytechnical Institute; UDC 669.3.053]

[Abstract] Laboratory tests were conducted with high-temperature (above the m.p. of sulfur) sulfuric-acid leaching of copper matte in an autoclave in the presence of surface-active agents, for comparison with already published data on the low-temperature variant of this process. In 2 hours processing time, 97-98% Cu and 8-10% Fe were extracted into solution which was suitable for subsequent precipitation of copper by hydrogen. In comparison with the low-temperature variant, it was found that high-temperature leaching of copper matte cuts the time of the process in half, reduces consumption of acid by 25-35%, lowers the amount of iron passing into solution by 20-30%, and provides for more stable process temperature conditions.

Peculiarities of Copper Fluoride Precipitation From Sulfate Solutions

927D0220D Moscow TSVETNYYE METALLY in Russian No 7, Jul 92 pp 20-21

[Article by A. D. Shinkarenko and V. I. Maltsev, "Ukrtsink" Plant and All-Union Research Institute of Nonferrous Metallurgy; UDC 669.536.23]

[Abstract] At the "Ukrtsink" Plant, a search for ways to improve the process for removal of chlorine from zinc solutions indicated that it was possible to dispense with the addition of copper sulfate solution. Industrial tests were conducted in which an agitator with volume of 45 cubic meters was filled with 30-35 cubic meters of solution to be treated, and 2-3 cubic meters of copper cake pulp. The mixture was then blown through with compressed air. The dependence of chlorine and copper content on the time that air was blown through the mixture was examined. It was found that after only 15 minutes, chlorine concentration in the zinc solution was reduced from 1.0-1.5 g/l to 200 mg/l while copper concentration increased to 0.76-1.9 g/l. It is expected that introduction of this process will eliminate the operation for regeneration of copper sulfate from copper chloride cake, will reduce the acid content of treated solution and the consumption of pure zinc oxide in hydrolytic purification of solutions, will reduce losses of zinc with copper chloride cake, and will result in labor and energy savings.

Behavior of Nonferrous and Noble Metals in Processing Electrolytic Slimes by the Method of Two-Stage Sulfation

927D0220C Moscow TSVETNYYE METALLY in Russian No 7, Jul 92 pp 17-20

[Article by V. M. Khudyakov, T. N. Greyver, V. D. Kim, Ye. V. Popkov, A. A. Kulakova, and I. L. Nikitina, Severonikel Combine and Mining Institute, St. Petersburg; UDC 669.33+669.243]

[Abstract] Data on results of introduction of a method of two-stage sulfation of platinum-containing slimes from electrorefining of copper and nickel are presented. The method was developed to overcome drawbacks of the methods of single-stage high-temperature sulfation and sulfating roasting and secondary electrolysis. The two-stage sulfation method is designed for selective extraction of nonferrous metals into solution in the first stage of sulfation, and then extraction of satellite metals of platinum, silver and tellurium in the second stage for the purpose of obtaining selective concentrates of noble metals. Based on the data from results of introduction of the method of two-stage sulfation, a number of advantages over the method of sulfating roasting and secondary electrolysis were demonstrated. First, the new method entails only one-half the technological operations, and the time of processing from the loading of slime to the obtaining of commercial concentrates is only one-eighth as long. Secondly, the new method keeps dust formation at a minimum, and losses of precious metals to dust amount to only 0.04%. Thirdly, the method's technology eliminates formation of solid recycle products such as slags which contain precious metals. With the two-stage sulfation method, direct extraction of platinum, palladium, rhodium, ruthenium, gold and silver from slimes into commercial concentrates is on a level of 98-99%, for iridium it is 95-97%, and overall the rate of extraction of noble metals, counting recycles, is more than 99%. In comparison with the method of single-stage sulfation at 300 degrees C, power consumption with the new method is less than half.

An Improved Mathematical Model of Autogenous Smelting of Sulfide

927D0220B Moscow TSVETNYYE METALLY in Russian No 7, Jul 92 pp 15-16

[Article by A. V. Tarasov, T. A. Bagrova, V. A. Kaplan, V. V. Galushchenko, State Scientific Research Institute of Nonferrous Metallurgy; UDC 669.33]

[Abstract] An improved mathematical model was developed for optimizing process parameters of flash smelting of copper sulfide ore. Calculations were made for steady-state operation of the smelter aimed at obtaining smelted products with an even composition. In the model that was developed, instead of matte copper content, copper content in sulfide suspension was taken as the independent variable. Results showed that calculation with this model makes it possible to predict the copper content in slag from flash smelting with an accuracy to within 10-13%, whereas calculations using a model developed by Japanese metallurgists indicated a slag copper content that was in fact two to four times less than the actual content.

Development of a Process for Autoclave Oxidation Leaching of High-Sulfur Nickel-Pyrrhotite Concentrate

927D0220A Moscow TSVETNYYE METALLY in Russian No 7, Jul 92 pp 9-13

[Article by N. P. Abramov, Norilsk Mining and Metallurgical Combine; UDC 669.243:66.046.8]

[Abstract] Research was conducted to determine optimum conditions and process specifications for breaking down

high-sulfur nickel-pyrrhotite concentrate which is obtained as a result of improved technology for enriching copper-nickel ore at the Norilsk Mining and Metallurgical Combine. The main goal of the research was to come up with a leaching process that prevents liquid sulfur from wetting sulfide minerals and thus forming sulfur-sulfide cake, which interferes with the autoclave process and necessitates frequent shutdowns. At the present time, a surface-active agent—lignosulfonate—is used to prevent this condition in breaking down pyrrhotite concentrate at the combine; with a high content of nickel and copper sulfides in concentrate, however, the rate of oxidation of sulfides is decreased and dissolving time is increased substantially. Research was conducted in three directions: study of the effect of grain size of crushed concentrate on the rate of leaching and consolidation of sulfur-sulfide conglomerates; study of the effect of solid emulsifying agents of sulfur (calcium sulfate, ferric oxide); and study of different surface-active agents (in addition to the currently used lignosulfonate, polymeric thioethers, including two types of sufane, were tested). Experiments in a laboratory autoclave showed that the use of sulfane as a surface-active agent is effective. With it, stable granules instead of sulfur-sulfide cake are formed in the leaching of both finely ground and coarsely dispersed concentrate. It was concluded that processing of high-sulfur nickel-pyrrhotite concentrate according to a hydrometallurgy scheme is possible either with a high degree of grinding of the raw material (100% to grain size of 44 micrometers and smaller) or with the use of sulfane as a surface-active agent. In the latter case, leaching takes place with the formation of sulfur granules which can be sent directly to sulfur smelting immediately after the leaching operation.

Structure and Plasticity of Ni-Ca Alloy Ingots

927D0190M Moscow TSVETNYYE METALLY in Russian No 5, May 92 pp 62-64

[Article by I. V. Meshchaninov, A. F. Plakhushchaya, R. M. Fridlyanskiy, S. G. Khayutin, State Research Institute of Alloys and Working of Nonferrous Metals; UDC 669.24'891-17]

[Abstract] The main difficulty in producing nickel alloys with 0.05-0.15% calcium for making the bases of oxide-coated cathodes is the poor workability of these alloys for hot rolling. Their plasticity drops sharply as the calcium content increases. A study was made of the effect of the structure on plasticity of the alloy in the cast state and after hot deformation.

It was determined that an important result of recrystallization from hot deformation is that boundaries of cast grains saturated with precipitates of the excess phase are enclosed inside new grains with comparatively clean boundaries. The formation of grain boundaries which are free of precipitates accounts for the higher plasticity after hot deformation. Also, hot deformation is accompanied by slipping of grains along boundaries and their migration. Blocking of boundaries by precipitates is an obstacle to slipping and migration, with the result that cracks may form. The creation of a system of "new" grain boundaries as a result of recrystallization, along which slipping occurs without cracking, leads to higher plasticity.

Obtaining Germanium Single Crystals by the Czochralski Process in a Magnetic Field

927D0190J Moscow TSVETNYYE METALLY in Russian No 5, May 92 pp 49-51

[Article by O. M. Alimov, I. N. Voronov, L. A. Gorbunov, D. A. Zaynalov, and L. N. Tityunik, State Research Institute of the Rare Metals Industry; Institute of Physics, Latvian Academy of Sciences; Scientific and Production Association of the Experimental Research Institute of Metal-Cutting Machine Tools; Solikamsk Magnesium Plant; UDC 669.782]

[Abstract] It is pointed out that modern microelectronics needs semiconductor single crystals with a radial uniformity of the doping agent on a level 1-3%, but such crystals cannot be produced by traditional methods such as the Czochralski process due to difficulties involving heat exchange and hydrodynamic flows in the melt. Results of experiments are presented which investigated the effect of technological parameters of the Czochralski process on radial non-uniformity of electrical resistivity in conditions of a constant magnetic field acting on the melt, and also in conditions of a constant magnetic field and electric current acting jointly on the melt. Germanium single crystals were grown in a Redmet-10 type unit which was equipped with a magnetic device for producing an axial-symmetrical field with magnetic induction in the center of the system of up to 0.215 T, and with systems for supplying and controlling direct current and measuring the temperature of the melt. The growing process was conducted in an argon atmosphere at a pressure of 20.2 kPa. The growing rate was 0.8 mm/min. The obtained single crystal specimens were examined for radial non-uniformity of electrical resistivity in cross section. For the selected parameters of crystal growing and parameters of the magnetic field and electric current in the experiments, the radial non-uniformity of electrical resistivity in the specimens demonstrated a rather wide range of values, from 24 to 2.2%. It was concluded that it is possible to obtain uniformly doped germanium single crystals with radial non-uniformity of electrical resistivity as low as 2.2% by employing a vertical magnetic field under optimal temperature conditions in the Czochralski process.

Resistance of Refractory Compounds in Cryolite-Alumina Melts and Aluminum

927D0190H Moscow TSVETNYYE METALLY in Russian No 5, May 92 pp 34-36

[Article by Yu. V. Borisoglebskiy, M. I. Karimov, M. M. Vetyukov, and S. N. Akhmedov, Leningrad Polytechnical Institute; UDC 669.7.018.45]

[Abstract] Results of thermodynamic calculations of the process of interaction of refractory compounds with cryolite-alumina melts and aluminum are presented. They established the following order of components of cryolite-alumina melts in increasing corrosiveness: $NaF<AlF_3<AlF<Al$-molten. Refractory compounds were found to be in the following orders of increasing resistance: $TiN<TiC<TiB_2$, and $ZrN<ZrC<ZrB_2$. Ti compounds were found to be more resistant than Zr compounds. To confirm the results of calculations, experiments were conducted to determine the solubility of refractory compounds

in cryolite-alumina melts and aluminum by chemical analysis. The refractory compounds were held in a cryolite-aluminum system at a temperature of 1273 K with subsequent quenching. The electrolyte and aluminum were analyzed for titanium content. Results of the thermodynamic calculations confirmed previously published studies indicating that aluminum present in electrolyte plays the decisive role in destruction of refractory compounds. In conducting experiments, the presence of dissolved aluminum in the electrolyte is a necessary condition, because in industrial baths molten aluminum is always present together with electrolyte. Thus, the experiments fully confirmed the thermodynamic calculations. Resistance of refractory compounds in cryolite-alumina melts and aluminum decreases in the order TiB_2, TiC, TiN, and introduction of metallic aluminum decreases the resistance of refractory compounds.

Effect of Composition of Nepheline Raw Material on Extraction of Aluminum Oxides and Alkalis in Processing Nepheline-Limestone Charges

927D0190G Moscow TSVETNYYE METALLY in Russian No 5, May 92 pp 27-31

[Article by B. I. Arlyuk, N. A. Zenkova, and T. V. Gorbacheva, All-Union Institute of Aluminum and Magnesium; UDC 669.713]

[Abstract] Methods were developed in the laboratory to model processes of sintering of charges and leaching of sinters to determine the dependence of extraction of aluminum oxide and sodium and potassium alkalis from sinters on the composition of nepheline raw material, as well the dependence of the charge-sintering temperature on the material's composition in production conditions. Extensive data were compiled on the chemical compositions of alumina-containing raw materials from a number of locations, and on the chemical compositions and properties of sinters made from the different raw materials. As a result of the studies, approximate quantitative dependences were established for the extraction of aluminum oxide and sodium and potassium alkalis and for the sintering temperature with respect to the composition of nepheline raw material having the alkaline ratio $R_2O:Al_2O_3 > 0.76$. Extraction of aluminum oxide increases the higher the content of Al_2O_3 is in the sinter and the lower the content of Fe_2O_3 is. Extraction of sodium alkali increases as the ratio of $Na_2O:SiO_2$ increases in the sinter. Extraction of potassium alkali depends on the mineral composition of the raw material; when the potassium content is mainly in the form of feldspar, it increases the higher $K_2O:SiO_2$ is, and when the potassium content is in the form of calcilite and secondary minerals of nepheline, it increases the lower $K_2O:Fe_2O_3$ is. The charge-sintering temperature decreases the higher $Fe_2O_3:Al_2O_3$ and $Na_2O:R_2O$, which determine formation of the melt, are.

Development of a Continuous Converting Technology for Copper Matte

927D0190E Moscow TSVETNYYE METALLY in Russian No 5, May 92 pp 16-19

[Article by F. A. Myzenkov, V. V. Mechev, O. V. Glupov, and A. I. Tertichnyy, State Research Institute of Nonferrous Metals; UDC 669.33]

[Abstract] Factors are discussed which have kept traditional converting technology for copper matte from being made a fully closed-cycle, continuous process, and a new method for continuous converting using top blowing is described. The method is based on studies of converting conditions in a two-layer system (slag-blister copper), in which 50-60% copper matte is converted autogenously with oxygen enrichment of 23-28%. Pilot-scale tests of the method were conducted in a vertical converter at the State Research Institute of Nonferrous Metals in Ryazan. Parameters of the process were investigated and different slags were tested to determine which ones allow converting of complex systems with top blowing. The slag that was found to be best suited for this process is rich in calcium oxide (23-30%) and low in silica (3-8%). The technology that has been developed calls for converting in a stationary converter with top blowing and continuous removal of gases containing 17-22% SO_2, which are captured for sulfuric acid production. Considering that gases from the continuous coverter process stage will have a SO_2 concentration of 18-20%, and gases from melting of the concentrate at least 30%, the resulting technology qualifies as an environmentally clean one that captures 93-97% of sulfur from the ore. The process is said to have advantages over the Mitsubishi process in that rich matte can be produced in more efficient converters.

Extraction of Rhenium From Sulfate Slimes at the Dzhezkazgan Copper Smelter

927D0190D Moscow TSVETNYYE METALLY in Russian No 5, May 92 pp 14-15

[Article by A. A. Kokusheva, G. A. Dayrabayeva, A. Sh. Usabekova, and N. A. Perfilyev, Scientific and Production Association "Dzhezkazgantsvetmet"; UDC 669.849:669.33]

[Abstract] Results of laboratory studies and industrial trials of rhenium extraction from sulfate slimes at the Dzhezkazgan Copper Smelter are presented. It was found that when no oxidizing agent is used, sulfuric acid leaching of rhenium yields only 35-40% of the Re content of the slime, but oxidizing agents can increase the yield. For example, use of potassium permanganate increases the Re yield to 85%, and potassium bichromate to 96%. They are costly, however, and manganese concentrate, which is readily available at the Dzhezkazgan ore deposit, increases the Re yield to 70-72% at only a small fraction of the cost of the other two oxidizing agents. Another key factor in the Re yield is the process temperature: raising the temperature from 30 to 90 degrees C increases the yield by 150%. Ninety degrees was found to be optimum, because higher temperatures cause strong evaporation of solutions and consume more electricity. The amount of oxidizing agent used also has an optimum level: if the amount exceeds 10% by weight of the slime, undesirable impurities enter the solution. Thus, sulfuric acid leaching of rhenium into solution from slime was found to have a maximum yield under the following conditions: process temperature 90 deg. C; ratio of solid to liquid components 1:5; sulfuric acid concentration 200-250 g/l; time of leaching 2 hrs; consumption of oxidizing agent 10% of weight of slime. Under these conditions 70-72% of Re passes into solution.

Economic Questions of Creating Waste-Free Metal Producton Technology at "Dzhezkazgantsvetmet"

927D0190C Moscow TSVETNYYE METALLY in Russian No 5, May 92 pp 12-14

[Article by A. Yu. Khokhlov, T. M. Abdrakhmanov, V. S. Pyzhov, and N. M. Mantsevich, Moscow Institute of Steel and Alloys, State Research Institute of Nonferrous Metals, Scientific and Production Association "Dzhezkazgantsvetmet"; UDC 669.33]

[Abstract] A key element in new technology being implemented at the Scientific and Production Association "Dzhezkazgantsvetmet" is processing of converter slag in a separate depletion furnace. Improvement of this process will allow more nonferrous metals to be extracted as commercial by-products of copper smelting. The problem of separating lead and zinc from the dust formed in different process stages was complicated by the fact that converter slag from the association's copper smelter contains quantities of lead and zinc that are rather close (5-10% and 4-5%, respectively). A large number of versions of converter slag depletion in an electric furnace were investigated, and three possible versions have been proposed: a) using Waelz slag from zinc production and flotation extraction of copper at an existing concentrating mill; b) using Waelz slag and extraction of slag iron into a sulfide phase; c) using Waelz slag and zinc-containing products from one of the association's concentrating mills (zinc concentrate, copper-zinc middlings). From the standpoint of quality of sublimates, the latter proved to be the preferable version. But one must consider economic factors related to the changing composition of ores going to smelting, costs of environmental pollution, and costs of new capital equipment and its operating costs. Economic indicators taking these factors into account were assessed, and their relative weights for the three different versions of converter slag depletion are presented in tabulated form. They are offered for a comprehensive technological-economic analysis leading to a final choice of one of the versions of converter slag depletion.

Sulfur Production From Autogenous Smelting Gases by the Methane Method

927D0190B Moscow TSVETNYYE METALLY in Russian No 5, May 92 pp 10-12

[Article by O. G. Yeremin, D. F. Makarov, A. A. Baryshev, V. N. Orlov, M. V. Timoshenko, and G. A. Yeremina, State Research Institute of Nonferrous Metals and Norilsk Mining and Metallurgical Combine; UDC 661.218]

[Abstract] The Norilsk Mining and Metallurgical Combine is using a methane method for producing sulfur from smelting gases. A comparative analysis was made of theoretical and experimental data on high-temperature reduction of sulfur dioxide by methane in an operating industrial reactor. Theoretical data indicated that the degree of conversion of sulfur dioxide into elementary sulfur depends on the temperature in the reactor and the consumption of natural gas. Data on actual operation of the industrial reactor over 157 workshifts were amassed showing the degree of conversion under high-temperature reduction at different reactor temperatures and levels of natural gas consumption. Comparison of the theoretical data and data of actual operation showed that the maximum possible degree of conversion (55-60%) is achieved at a temperature in the reaction zone of 1250-1300 degrees C and a coefficient of reduction of 5- 6, which is reached if the consumption of natural gas is increased by 15-20% in comparison with the stoichiometric level. The obtained data have practical significance for selecting optimum operating conditions of the reactor with subsequent processing of reduced gases in a Claus catalytic reactor. Maximum sulfur yield is achieved with repeated reduction of sulfur dioxide in the original gas by 15-20%. By supplementing the process with a hot catalysis stage for processing sulfur and carbon oxides, a lesser degree of repeated reduction of sulfur dioxide in the high-temperature reactor is required. As a result, less natural gas is consumed, the process is made more economical, and total yield of sulfur from smelting gases is higher.

Degradation Processes in Silicon Carbide Refractories Exposed to a High-Temperature Gas Stream

927D0208A Moscow OGNEUPORY in Russian No 2, Feb 92 pp 2-6

[Article by A. K. Karklit, All-Union Institute of Refractories; UDC 666.762.852.001.4]

[Abstract] Degradation processes were studied in silicon carbide refractories exposed to high-temperature gas streams. Fired and unfired specimens were made from powders with grain sizes ranging from Nos. 3-125. The fired specimens were made with either a silica or a nitride binder, or they were siliconized (10-15% carbon in the refractory mass and firing in silicon vapors), and silica glass, bentonite, ferrosilicon, and boron carbide were added to impart strength to the silica binder and inhibit SiC oxidation. The unfired specimens were made with Bakelite binder polymerized at 180-200°C. Specimens of each type of refractory with select physical and mechanical properties were tested in a high-temperature (2650-2730 K) and velocity (2300 m/s with a 1.2 air-fuel ratio) gas stream created by igniting alcohol in oxygen (nearly 13% O_2). Test duration was 15 s, which is much shorter than usual for this type of test. The specimens were cylindrical, 50 mm long and 20-25 mm in diameter. Change in specimen height during the 15-second test period was recorded photographically. Oxidation of the SiC with the formation of SiO, SiO_2, and CO was the main process resulting in a dramatic alteration of the composition and properties of the specimens in the layer below the one exposed to the gas stream. The degradation processes occurred at the fastest rate within the first 5 s, after which the rate stabilized. The silica binder specimens had the greatest specimen height and mass loss rates (0.88 and 1.92 average specimen height loss, in mm/s, and degradation rate, in kg/sq m x s, respectively), followed by the siliconized specimens (0.85 and 2.46) and those made with the nitride (0.77, 1.81) or Bakelite binder (0.68, 1.63). The latter also had less SiC oxidation and a correspondingly lower proportion of SiO_2 in the layer concerned. Figures 9, tables 5; references 9: 7 Russian, 2 Western.

Alloying Silicon Carbide Components With Aluminum During the Process of Siliconizing Firing

927D0208B Moscow OGNEUPORY in Russian No 2, Feb 92 pp 6-9

[Article by S. V. Kazakov, A. S. Rabinovich, and A. S. Kheyfitz, All-Union Institute of Refractories; UDC 666.762.852.017:620.187]:621.762]

[Abstract] The alloying of silicon carbide components with aluminum was studied to determine its effect on component structure and electrical properties. Three tubular specimens were extruded from an 85 wt. % primary SiC (SiC') mass and fired in a siliconizing packing at temperatures between 1900-2200°C for 5.5 to 6 h in a resistance furnace. During firing, the specimens were arranged in a symmetrical fashion relative to the tubular graphite heating element. Sintering of the green extrusions and structural formation was more readily effected by the addition of process carbon to the raw material and by the formation of carbon residue released during thermopyrolysis of the binder. These carbons, together with the carbide-forming elements present in the packing, helped to form secondary SiC (SiC''). In order to alloy the SiC with aluminum, an aluminous substance was also added to the packing. After they had cooled, the specimens were fired a second time. It was found that this method of forming SiC components creates a layered structure in which SiC'' grains are alloyed with aluminum, and that this structure promotes consistent electrical resistivity throughout the component cross-section. The degree of alloying can be monitored by X-ray microspectrometry. Electrical resistivity can be estimated within the framework of a generalized model of conductivity in a multicomponent medium, in which SiC'' forms a continuous matrix, and SiC' grains make up a discrete phase. Figures 2, tables 1; references 11: 9 Russian, 2 Western.

Role of Sintering Additives in Lime Refractory Production Technology

927D0208C Moscow OGNEUPORY in Russian No 2, Feb 92 pp 13-16

[Article by R. M. Bezikova, Leningrad Institute of Technology Central Weather Bureau, G. I. Kuznetsov, and V. M. Gropyanov, All-Union Institute of Refractories; UDC 666.762.62.046.44]

[Abstract] A new lime refractory production process that utilizes titanium oxide as the sintering additive was proposed. TiO_2 was selected because the eutectic temperature of CaO-TiO_2 is 2010 K and because calcium titanates are resistant to atmospheric hydrolysis. The refractory is made by pulverizing pure or esp. pure calcium carbonate to a particle size of 100-150 μm and adding 2-6% TiO_2 or 2-4% titanium ferrite. (Optimum additive percentage was determined empirically.) A 5-% aqueous solution of sulfite waste liquor with a density of 1.15 g/sq cm is used as the binder. The green mass is then pressed into briquets and fired at 2020 K. The lime refractory material has an apparent density of 2.75-3.03 g/cu cm, apparent porosity of 3.4-9.8%, compressive strength of 60-140 N/sq mm, and a loaded deformation temperature of 1610 to 1700°C or higher. Figures 5, tables 1; references 5: Russian.

Uses for Non-Destructive Methods of Refractory Quality Control

927D0208E Moscow OGNEUPORY in Russian No 2, Feb 92 pp 21-23

[Article by V. A. Kononov, Rosogneupor, and S. V. Martynenko, Central Scientific Research Institute of Ferrous Metallurgy; UDC 666.76.017:620.179.16]

[Abstract] Non-destructive methods of assessing the physical and mechanical properties of refractory products are being more widely used in place of destructive testing methods throughout the refractories industry and by end-users of refractory products to ensure 100% quality control. The Novomoskva refractories plant is using x-ray analysis to detect inclusions, variation in wall thickness, graphite distribution, and internal defects such as cracks and splits in the refractory components of continuous casting machines. Radio-frequency inspection methods are being used primarily to measure porosity. Various acoustical methods, such as the shadow and echo methods and acoustical emission,

are being used extensively by U.S., Japanese, and European firms for specific applications. For example, acoustical emission is being successfully used to assess deformation and destruction mechanisms and heat resistance. The echo method is used to detect internal cracks and cavities and to measure wear and the useful thickness of linings in thermal processing equipment. Ultrasound is being used in conjunction with physical measurements to measure the strength of a refractory material or product. Acoustical resonance is being used at the Vnukov refractories plant to measure density, porosity, and the mechanical strength of the plate linings of slide valves. These methods are highly accurate and reproducible and enable refractories producers to effect substantial savings in quality control costs while enabling end-users to avoid costly equipment failures. Figures 3; references 15: 11 Russian, 4 Western.

Electrical Conductivity of CeO_2-Ta_2O_5 Ceramics in Air and Combustion Gasses

927D0208D Moscow OGNEUPORY in Russian
No 2, Feb 92 pp 19-21

[Article by F. A. Akopov, B. M. Barykin, G. Ye. Balyano, Yu. D. Novov, and Ye. P. Pakhomov, Institute of High Temperatures of the USSR Academy of Sciences; UDC 666.762.6.017:537.311.3]

[Abstract] Cerium dioxide-tantalum oxide ceramic material was studied to determine the combined effects of a gaseous atmosphere and the tantalum oxide alloy on its electrical conductivity. More than 99.8% pure cerium dioxide and tantalum oxide powders were mixed to form compositions in which the proportion of tantalum oxide was 0.5, 2.3, or 5%. The powders were then briquetted, fired at 1870°C for 5 h to synthesize a solid solution, and re-pulverized to obtain fractions from 0.65 to less than 0.05 mm. Bar-shaped specimens 7 x 7 x 70 mm were compacted at 100 N/sq mm from tri-fraction mixtures of the powders and fired at 1820 K for 6 h. The fired specimens had an apparent porosity of 18-20% and a total porosity of 20-22%. Electrical conductivity was measured with four PR-30 platinum-rhodium probes utilizing direct current. In the first series of tests, the specimens were exposed to atmospheric air, and in the next series of tests, to an atmosphere of combustion products created by igniting propane in oxygen at air-fuel ratios of 0.7, 0.9, and 1.2. It was found that alloying cerium dioxide with tantalum oxide greatly increases the material's conductivity in air (to the solid solution saturation point). Unalloyed cerium dioxide ceramics exposed to combustion products have a much higher electrical conductivity than those exposed to atmospheric air. Moreover, the lower the air-fuel ratio, the higher the conductivity. Alloying cerium dioxide lowers the sensitivity of the conductivity of this material to the composition of the gaseous atmosphere of combustion products, especially for saturated solutions of tantalum oxide in cerium oxide. Figures 4; references 3: Russian.

Testing Refractories Used in an Experimental Vessel for Acid Oxygen-Process Steelmaking

927D0208G Moscow OGNEUPORY in Russian
No 2, Feb 92 pp 31-33

[Article by V. I. Drozd, V. L. Bulakh, S. N. Romanenko, Ukrainian Scientific Research Institute of Refractories, R. V. Starov, and M. N. Yednak, Institute of Ferrous Metallurgy; UDC 666.762.2:[669.184.244.66:669.184.225.4]

[Abstract] Experiments were performed to determine the factors affecting the service life of dinas linings in oxygen-process steelmaking vessels. Laboratory specimens were formed from 100% Ovruch quartzite on a laboratory hydraulic press under 50 N/sq mm of pressure and fired at 1360, 1380, and 1420°C for 6 h to effect different degrees of quartz degeneration. Two different compositions, No 1 and No 2, were formulated, depending on the additives used in the refractory mass. For both compositions, density decreased while apparent porosity and compressive strength increased as the firing temperature increased. The greatest proportion of residual quartz was found in the refractory compositions fired at 1360°C, and dinas No 1 had more residual quartz than dinas No 2. Therefore, dinas specimens fired at this temperature were used throughout the rest of the study. Thermal resistance was determined by measuring the thermal expansion coefficient, thermal conductivity, bending strength, and shear modulus of the dinas at temperatures ranging from 20 to 1300°C. These data showed that the thermal resistance of the specimens sharply increased as the average temperature increased, especially at temperatures above 600°C. Moreover, dinas No 1 had greater thermal resistance than dinas No 2. The slag resistance of the dinas specimens was then tested by drilling a hole through the center of the cube-shaped test specimens, heating them in a Kryptol furnace to a temperature of 1670°C, and allowing melted slag of typical composition to drip through the hole. The same test was performed on specimens of DM industrial dinas and MKV-72 mullite-fused alumina. The specimens were then cross-sectioned and the area of slag impregnation measured. Dinas No 1 specimens had the greatest slag resistance; 25% of their area was penetrated by the slag. Dinas No 2 specimens had 30% of their area penetrated by slag, and the other refractory specimens were completely impregnated. Petrographic analysis of specimen cross-sections revealed the presence of a distinct three-zone structure consisting of a least-changed zone, a transitional zone, and a reaction zone. The experimental data were used by the Krasnogorov refractories plant to manufacture a test batch of standard-size dinas lining materials, which were tried out in the 0.3-t laboratory steelmaking vessel at the Institute of Ferrous Metallurgy. Blowing time was 10-12 min., and the average post-blowing melt temperature ranged from 1600 to 1720°C, averaging 1660°C. In comparison with the DM dinas and MKV-72 linings, dinas No 1 proved to have the greatest overall resistance to the erosive effects of the blowing process in every respect and in nearly every section of the vessel, except for the cylindrical part and the throat, where the MKV-72 was better. The dinas lining also eroded more uniformly than the other linings. The lining wear pattern was typical for that of oxygen process steelmaking vessels.

Depending on process temperatures and times, the maximum wear rate of dinas linings should be comparable to that of basic refractory linings. It is anticipated that considerable economies in raw materials and improvements in steel quality will be realized by converting to acid refractory linings such as dinas in oxygen-process steelmaking. Figures 2, tables 5.

Materials Based on Carbon Fibers

927D0212A Moscow TEKHNIKA I VOORUZHENIYE in Russian No 1-2, Jan-Feb 92, pp 10-12

[Article by R. Levit, professor, doctor of technical sciences, L. Fridman, professor, doctor of technical sciences: "Materials Based on Carbon Fibers"]

[Text]

...in Engineering

Efforts to develop carbon fibers began with research by Edison and his contemporaries on developing incandescent carbon filaments for electric light bulbs. These first specimens of a new type of material had low stress-strain indicators, high brittleness, porosity, oxidizability and other drawbacks. After carbon incandescent filaments in electrical equipment were replaced with tungsten, they were forgotten for a long time.

In the 1950's carbon fibers were essentially rediscovered in connection with the acute demand from space technology and aviation for light, high-heat structural and heat-shielding materials. High-quality carbon fibers were produced almost simultaneously in the USA (on the basis of viscose fibers in cyclic polybutylene) and in the USSR (on the basis of polyacrylonitrile fibers), and somewhat later in other countries. Modern carbon fiber materials, developed on the basis of the latest advances in polymer chemistry and physics and chemical fiber engineering, are far superior to their predecessors in terms of their properties. Various kinds have been produced with unique stress-strain, thermal, electrophysical and other properties. Today one can already speak about several classes of these fibers which, depending on purpose, have specific well developed consumer properties. Different countries are now producing carbon fiber materials on an experimental scale for construction purposes with a strength to 500 kgf/mm^2. In the near future it is expected to increase by at least 20-40 percent.

The raw material for producing carbon fiber materials in industry are polyacrylonitrile or viscose (hydracellulose) fibers, as well as fibers formed from specially prepared petroleum pitches. The processes for producing carbon fiber materials from various kinds of raw materials include several stages. First raw fibers are produced or prepared and, if necessary, various fiber structures are formed from them (textile and non-textile). Then the raw material is prepared for carbonization. Depending on the type, it undergoes thermo-oxidative stabilization or processing with substances such as antipyrenes. Other processes are possible.

Carbonization involves heat treating raw fibers without access to air (or in neutral or reductive media), usually at temperatures to 800-1000°C. In some cases heat treatment is done very slowly according to a complicated heat regime. The process of high-temperature treatment is carried out at temperatures of 1500-2500°C.

Another way to produce textile industrial materials from carbon fibers is to process ready-made carbon threads or cut carbon fibers by weaving or re- processing into non-textile materials, paper, and other composite materials.

When raw polymers are carbonized, complicated chemical and physical processes take place in them which lead to a fundamental change in the constitution and structure of the substances being processed. The result is a carbon, and at a higher temperature (2000°C or higher) a graphite-like polymer. The latter is distinguished by the fact that, between the parallel aromatic "parquet-like" planes which are joined into "real" graphite by relative weak molecular forces, in this case there form strong "strands"—chains of carbon atoms which keep the planes from slipping relative to one another. Because of these bonds the graphite-like fibers have stress-strain indicators superior to those of small-crystal graphite. Bundles of parallel "parquet-like" planes (crystallites) forming graphite-like structures such as "bands" in combination with "amorphous" layers are oriented primarily along the fiber's axis. The higher the degree of orientation and the fewer the defects in the resulting crystallites, the stronger the resulting carbon fibers.

The term "carbon fibers" encompasses partially carbonized (heat treatment at temperatures to 500°C, carbon content to 90 percent), carbon (500- 1500°C, 90-99 percent) and graphitized (above 1500-2000°C, more than 99 percent) fibers. In addition, carbon fiber materials are classified in terms of application and level of stress-strain properties. In terms of the first characteristic, they can be broken down into four groups: structural, heat-shielding, with controllable electrophysical and physicochemical properties (adsorbents, catalysts, filters, antifriction materials, etc.). In terms of the second, with regard for the Young's modulus and strength modulus achieved in the fiber, most researchers divide fibers into high-modulus, high-strength, and low-modulus ("soft"). Sometimes they identify medium-modulus as a separate group.

Because of their high price, high-strength, and high-modulus carbon fibers have found limited applications. They are basically used in the aerospace industry, as well as for manufacturing the reinforcing fiber base for light and strong structural composite materials. Fibrous composite materials are a combination of a polymer, metal, and ceramic matrix with the fiber or fiber structure that fills it. The degree of fill reaches 60-65 percent of the volume. In terms of their specific stress-strain properties, these materials are far superior to both traditional metal materials and to proven especially high-strength grades of fiberglass and glass-reinforced plastics.

Composite materials made of carbon fibers are widely used in prospective airplanes and missile technology. Their use makes it possible to reduce airplane mass 20-25 percent and the cost of production by 5-10 percent. As early as 1981 a new experimental eight-seat airplane whose fuselage was almost entirely made of a structural material based on the carbon fiber "tornel" was successfully tested abroad. The savings in mass compared to metal were 40 percent. As output of the promising materials increases, the process for producing them is improved, and their cost lowered, there is no doubt that they will have a bright future not only in the defense, but also in other industries.

Soft (low-modulus) and medium-modulus carbon fibers and materials made from them, which are already being intensively introduced into various areas of technology and everyday life, are extensively used in the national economy.

The "Khimvolokno" Leningrad Scientific Research Institute has been giving particular attention to developing precisely this class of fibers (uglen, gralen, evlon, concor, VDE, etc). Together with related enterprises ("Bumprom" All-Union Scientific Production Association and others) they are developing and introducing various carbon fiber materials and products. The basic advantages of medium-modulus and, especially, soft carbon fibers (in addition to relatively low cost) are increased elongation and flexibility, low brittleness, and soft feel. Because of these properties, they can be introduced as active filler into structural materials without major crushing during production and use. This is especially important in producing materials for the electrical and radio engineering applications and in using carbon fibers as antistatic additives.

...In Ecology and Medicine

One of the unique features of our times is that we are surrounded by harmful substances which have a significant action on the human body, even in small concentrations. Granulated adsorbents widely used to neutralize them (usually activated carbons) do not satisfy modern requirements for adsorption and desorption rate or capacity when the substances to be absorbed are in small concentrations.

Successes in developing and setting up production of carbon fibers which have substantially lowered their cost have made it possible to create a new kind of adsorbent based on them—carbon fiber adsorbents with small-diameter (6-12 microns) elementary fibers, a controllable, homogeneous microporous structure, and reactive chemical groups on the surface. The new chemicals have adsorption and desorption rates and capacities for small concentrations of substances that are several times higher than granular adsorbents. They have no toxic, irritant, or allergenic properties, which encourages their extensive use for a variety of purposes.

The first patents on obtaining these adsorbents were registered at the beginning of the 70's. Among the first in our country were LenNII "Khimvolokno" and the Institute for General and Inorganic Chemistry of the Belorussian Academy of Sciences, who joined efforts to perform research in this field.

Fibers based on hydrated cellulose and polyacrylonitrile were used to produce carbon fiber adsorbents. The micropore volume on the resulting adsorbents was 0.6-0.7 cm^3/g with a narrow range of sizes. Furthermore, the micropores are directly connected to the outer surface of the fiber, not through transport pores as is the case in granular active carbons.

Because of the small diameter of the new adsorbents' elementary fibers (6-12 microns) their external geometric surface (disregarding the pore surface) is 2-2.5 m^3/g, while this parameter is only 0.002 m^3/g in the finer-grained adsorbent SKS, which consists of spherical particles 800 microns in diameter.

The specific active micropore surface of the carbon fiber adsorbents is 800 mg. Adsorbents activated in water vapor have the maximum surface; those activated in gas (CO_2), the minimum.

By changing the original polymer fiber, its processing conditions, the kind of activator, and the degree of activation, specialists were able to control the porous structure and

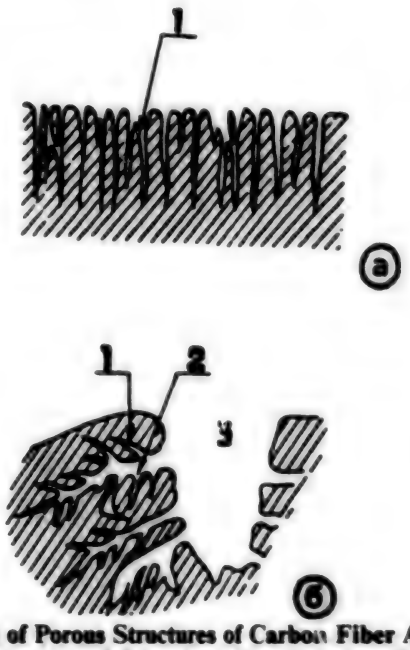

Models of Porous Structures of Carbon Fiber Adsorbents (a) and Granular Active Carbons (b)
Key: 1 - micropores; 2 - mesopores; 3 - macropores

chemical composition of the surface functional groups of carbon fiber adsorbents, thereby changing their adsorption properties and obtaining material with specific properties.

LenNII "Khimvolokno" has developed carbon fiber adsorbents in various textile forms. These are braids, staple, cloth, nonwoven materials, laces, cords, and threads. This diversity permits their extensive use for various purposes. The negligible hydro- and aerodynamic resistance of the materials, which is determined by their fibrous nature, has made it possible to design an adsorbing respirator in the form of nonwoven materials. In emergencies, to evacuate people from an area with a toxic atmosphere, carbon fiber napkins in the form of cloths or mats can be used. They are much cheaper and more readily available than gas masks.

Studies have shown that the process of adsorbing vapors and dissolved benzene, acetone, carbon disulfide, and other organic substances with carbon fiber adsorbents takes place at a high speed exceeding the figure for granular carbons by a factor of 2.5-3. This unique property can be used to purify water, including to remove disease-causing microorganisms.

The method developed by LenNII Khimvolokno to remove bacteria and viruses from water using activated carbon fiber increases the degree of water purity to 60.0 percent for viruses and 98.0-99.9 percent for bacteria (activated granular carbon, 40 and 9.2-37.3 percent). The high efficiency with which bacteria, viruses, and organic substances are adsorbed using carbon fiber sorbents is combined with simplicity of design and a reduction in the time required to purify the water.

This method is recommended for purifying water when there are no "pure" sources, as well as if water supplies must be stored for a long time. In the first case a special small filter bag including, in sequence, filtering, adsorption, and

protective layers or a carbon fiber adsorbent in a plastic case, is used. In the second case, one or several cartridges with the adsorbing substance are placed in the vessel for the entire required storage period.

The water purification filter has been used in the field to purify tap water, as well as water with a benzene concentration of 10 mgl. Purity was recorded in terms of oxidizability with potassium permanganate. The original tap water had an index of 4.16 before purification, which is considered "polluted" according to current standards. After purification of 1 liter of water, its index was 1.8 ("pure"). The water contaminated with benzene had an index of 15.68 before treatment and 2.6 after.

If large quantities of drinking water must be purified, another device can be used. It is a column 500 mm in diameter into which 35 kg of adsorbent are placed. Tap water with an oxidizability index of 4.16-5.6 was passed through the column at a rate of 1.5 m^3/h. The oxidizability index of the purified water was: after 1 hr of filtration, 0.72; after 21 hr, 0.86; after 48 hr, 0.90.

Carbon fiber adsorbents may be extensively used in medicine, primarily for rapidly removed poison absorbed into the blood. Hemosorption using the institute's developments is far superior in terms of the ability to remove many poisons from the blood to hemodialysis using an artificial kidney or other similar detoxification methods.

The use of carbon fibers as adsorbing layers in bandages and drainages in the treatment of wounds and burns has demonstrated the high efficiency of this bandaging material, especially when there is a large number of wounded, since its use makes it possible to prolong the pre-hospitalization period. These bandages are also effective in protecting the surface of a wound from toxic chemical and biological substances.

Preventive use of the adsorptive fiber "Vaulen," one of the developments of LenNII "Khimvolokno," increases the body's resistance to poisons several times. This is especially important in cases when it is necessary to send rescue teams into contaminated zones. All carbon adsorbents developed for medical purposes, together with the required documentation, have passed the technical acceptance of the USSR Ministry of Health and are permitted for clinical trials. These products are being made at LenNII "Khimvolokno" experimental plant.

St. Petersburg's "Khimvolokno" Scientific Research Institute Offers New Carbon-Fiber-Based Materials

UGLEN HEAT-RESISTANT ELECTRICALLY CONDUCTIVE FIBER—braid or staple (from 5 mm long), untwisted with adjustable conductive properties.

It withstands a temperature to 3000°C in an inert or reductive medium without significant loss of strength or weight; to 350°C in an oxidizing medium. The fiber is resistant to aggressive media and to solvents. It has a low ash content and is nontoxic.

The material is elastic and inexpensive compared to other known carbon fibers.

It is the optimum filler for various compositions. For example, it can be used to reinforce building materials. It is used to make heat-resistant and chemical-resistant composite materials which are not part of a structure; to produce new electrical and radio engineering materials: plastics, nonwoven materials, papers; to manufacture rigid and flexible heating elements at 36-220 V with a specific power to 1 kW/m^2 or more. It is being successfully used as an antistatic additive to various composite materials, plastic, synthetic leather, and rubber.

UGLEN is the basis for producing filtering, adsorptive, catalytically active, antifriction, and other materials.

GRALEN CARBON FIBER—a staple fiber or braid with regulated electrical conductivity. It has increased resistance to oxidation compared to most other carbon fibers. It withstands temperatures to 3200°C in inert and reductive media and to 450-500°C in an oxidizing medium. It has good adhesion to polymer binders in many classes. It can be used to produce various heat-resistant plastics. The material's low density permits it to be successfully used as an additive to form various polymers that are non-electrified at operating temperatures. Because of GRALEN's high electrical conductivity, this effect is achieved with minimum addition of fiber, which makes it possible to preserve the product's original paint.

It can be used to produce electrically conductive papers, as an integral part of graphite electrodes, in mixtures with various additives to replace asbestos in the brake blocks of cars and trucks, to make antifriction materials for bearing assemblies in automobile production, and in other machine building industries.

EVLON CARBON FIBER—heat-resistant electrically conductive carbon fiber with rated electrophysical indicators. It is nontoxic and non-explosive and difficult to ignite. It withstands temperatures to 3000°C in inert or reductive media without significant loss of strength or mass and to 350°C in an oxidizing medium.

It is intended for use as an electrically conductive filler (cut or in the form of textile structures) in papers, synthetic leathers, plastics, and rubber to give them antistatic properties or specified electrophysical characteristics. It can be used to produce filtering, adsorptive, and antifriction materials.

The use of the fiber as a reinforcing filler in composite materials increases their stress-strain characteristics.

LIKRON NONWOVEN CARBON MATERIAL—intended for making carbon plastics with electrical conductivity and increased chemical resistance. It may be used as a heat-insulating layer, as well as a protective liner in uniforms for people working with aggressive substances. It is nonflammable, nonexplosive, and nontoxic and withstands temperatures to 3000°C in inert and reductive media and up to 350°C in an oxidizing media.

LIKRON's electrical conductivity and chemical resistance, combined with its wide range of surface densities and the ability to obtain a final product in sheet form permit its use as a high-heat filler, antistatic, or electrically conductive layer. It can also be used to produce adsorptive and ion-exchange materials.

It has improved physicochemical and electrophysical properties, which made it possible to use it to create low-inertia

plate heaters with an operating temperature to 200-250°C (which is 100-150°C higher than when carbon fiber paper is used), as well as to develop more effective uniforms that are not ignited by phosphorus or metal spray (if they fall on the material, the temperature of the reverse side reaches 50°C in no less than 5-10 sec depending on its thickness.)

BANDAGE FOR TREATING WOUNDS AND BURNS—a sandwich consisting of a top and bottom layer of gauze and a thin inner layer made of carbon fiber adsorbent Aktilen-1. It is intended for treating infected wounds and burns and protecting the injured surface. It is used in surgical clinics and burn centers.

The bandage's use in several clinics in the USSR has prove the effectiveness of treating patients with various kinds of suppurative and inflammatory ailments. This bandage can be successfully used in first aid for the injured or burned surface of soft tissue to prevent the development of infection and toxemia. This is critical in the pre-admission and early hospitalization stages. The use of the bandages shortens the hospital stay by 1-3 days, which is important when treating large numbers of wounded.

Production of the material has begun at the NII "Khimvolokno" experimental plant, and a partner is being sought to set up commercial production of the bandage.

VAULEN ADSORPTIVE FIBER FOR ORAL USE (a substance for treating acute poisonings) is a dispersed carbon fiber adsorbent.

It has pronounced adsorption activity in relation to several highly toxic and pharmacological substances (organophosphorus compounds, chlorinated hydrocarbons, barbiturates, radionucleides, etc.) and does not irritate the mucous lining of the gastrointestinal tract.

VAULEN is 5-10 times better in adsorptive and kinetic parameters than the activated carbon KARBOLEN now used in medical practice to adsorb toxic substances.

In emergencies (spillage or discharge of highly toxic substances, etc.) it is used by victims to prevent severe toxic injuries.

The administration of a preliminary dose by rescuers significantly lowers the possibility of poisoning by toxic and radioactive substances in a contaminated zone.

The developer has started production of VAULEN in a limited quantity at contract prices. Joint production with an interested organization is possible in order to increase output of VAULEN powder and its packaging.

Send proposals to 195030, St. Petersburg, ul. Khimikov, d. 28, NII "Khimvolokno." Telephone (in St. Petersburg) 227-78-75.

Automated Design System for the Technical Documentation of Non-Ferrous Alloy Casting Production and Equipment

927D0235E Moscow LITEYNOYE PROIZVODSTVO in Russian No 5, May 1992 pp 24-25

[Article by V. M. Kolodkin, Udmurt State University, Yu. N. Isakov, and Yu. N. Perevoznikov, Izhev Foundry Plant; UDC 621.74:681.3.001.63]

[Abstract] A relatively simple and inexpensive automated design system for producing the technical documentation required for the die and investment casting processes has been developed. The documentation produced by this system meets the specifications of the Unified Technical Documentation System and includes all elements of a technical document. The system features a multi- level, menu-driven interface in a windows environment as well as dialog windows. The diagnostics hardware checks input for accuracy, logical correlation with previous input, and compatibility with the system's information retrieval resources. The technical documentation produced by the system is stored in its archives. Utilization of this system by industrial users revealed two trends. The first involved constant refinement of the information retrieval resources as designs, processes, equipment, materials, and so forth were modified. The second has to do with developing a graphics support capability using AutoCAD software written in AutoLISP. This system is designed to enable engineers to create drawings of mold components in a three-stage process. In order for this system to be successfully utilized, design engineers must be able to work in an AutoCAD environment. As the creation of a universal automated design system would probably be cumbersome and expensive, the recommended approach is to utilize specialized software, parametrizer, graphics editors, and so forth in the capacity of software tools that will enable engineers to work with an engineering data base built around mold drawings and components. This approach will cost the least amount of time and money and can be customized for a particular foundry. The CAD system described herein can be run on an IBM 286 PC with a math co-processor and a VGA or EGA monitor and has been used successfully at the Izhev Foundry. References 5: Russian.

Microarc Oxidation of Aluminum Alloy Parts

927D0235D Moscow LITEYNOYE PROIZVODSTVO in Russian No 5, May 1992 pp 19-21

[Article by K. A. Batyshev, ENIMS [Experimental Scientific Research Institute of Machine Tools]; V. I. Samsonov, and A. P. Arefyev (Ingeokom International Material Society); UDC 621.74.043:669.715]

[Abstract] The advantages of electrolytically oxidizing aluminum alloy parts were discussed. ENIMS has developed a safer oxidizing station that features an insulating transformer and a grounded electrolyte. The thickness of the oxidized coating can vary from 300 to 800 μm, depending on alloy type and composition, oxidation conditions, and so forth, which can be customized to suit the type of part being treated. The coatings are very hard and highly wear-and corrosion-resistant (corrosion resistance is 10 to 100 times higher than for uncoated parts), have a low friction coefficient, thermal conductivity that is 25 to 30 times lower than that of uncoated alloys, and low thermal expansion (8×10^{-1} deg^{-1}. They bond to the base metal so well that the yield strength of the coatings is virtually equivalent to that of the metal to which they are applied. Coating elasticity is 2.5 times higher than that of steel. Dielectric strength is 5 to 20 W/μm; insulation resistance is 10^8 ohms. The conditions under which some of these properties were tested were described. These coatings have been tested with excellent results on components such as the aluminum cooling boards used in electronics, hydraulic slide bearings, and the drive shafts of micro hydroelectric plants. There are plans to test them on components such as those in precision machine tools and nozzles exposed to abrasive wear. The drawbacks of this technology are: the brittleness of the coatings, which precludes their use in parts and components subject to high shock loads; the power requirements of the coating equipment, which can translate into a power output of 4 to 10 kW/sq dm and electricity consumption of 4 to 8 kW h/sq dm; and the fact that almost all of the electricity used is needed to heat the electrolyte, which leads to complications in cooling large parts. A systematic classification of coating type and application has been worked out. Tables 2.

Mathematically Modelling the Process of High-Speed Directional Crystallization

927D0235C Moscow LITEYNOYE PROIZVODSTVO in Russian No 5, May 1992 pp 16-18

[Article by M. M. Koroleva and S. V. Lobanov, Rybin Institute of Aviation Technology; UDC 621.746.628]

[Abstract] High-speed directional crystallization was mathematically modelled and the model experimentally validated to determine whether the high-speed directional crystallization of turbine blades could be improved. The model was constructed on a computer using the finite differences method and was based on a ZhS26-alloy casting that simulates the thermal behavior of shroud- ringed turbine blades. The program used to calculate the basic process parameters (crystallization rate, temperature gradient and cooling speed along the isoliquidus front, and the position of the two-phase region relative to the thermal elements of the casting station) was written in Fortran-IV. Casting conditions, which were described, were held constant. The results of the study led to the following recommendations: 1) Reduce the normalized size of the shroud flange by changing its shape, thereby reducing the length of the two-phase region and keeping it closer to the furnace, other conditions remaining unchanged; 2) optimize the casting process by (in order of importance): reducing the thermal resistance of the mold walls, reducing the temperature in the crystallization furnace, downsizing the dead space between the furnace and the coolant (i.e., raising the coolant level), increasing the liquid-metal coolant temperature and thereby improving its insulating effect, and reducing the casting withdrawal speed; 3) slowing down the rate at which the shroud flange is withdrawn until the shroud ring exits the furnace; alternatively, hold the casting in a position such that the shroud ring is located in the bottom furnace zone until the shroud flange begins to crystallize; 4) maintain the proper position of the isoliquidus front relative to the furnace exit by changing the casting's movement over time with the aid of automated process control equipment. If these recommendations are followed, structural defects, friability, and porosity in these castings can be avoided. Figures 3.

Investment Casting Equipment

927D0235B Moscow LITEYNOYE PROIZVODSTVO in Russian No 5, May 92 pp 9-10

[Article by A. P. Anikeyev, SKBTL [Special Design Bureau of Casting Process Technology]; UDC 621.74.045]

[Abstract] SKBTL has designed a great deal of versatile precision investment casting equipment that is in use at both small and large foundries at major automotive plants and other industrial enterprises. Unfortunately, the major producer of this equipment, Litmash, has gone over to the exclusive production of die-casting equipment. From 1989 to 1991, SKBTL, in cooperation with the Kharkov Affiliate of the All-Union Scientific Research Institute of Casting Equipment, worked to design and develop a 13-station production line of precision investment casting equipment that would be used to make the turbine blades for gas turbine engines. The design work and technical documentation were completed for five of the 13 stations: a station for preparing the mold pattern (model 62751); a station for straightening dried cores and assembling them in the mold box (model 62661); a station for removing ceramic from blade channels by immersing them in molten potassium bifluorides and ammonia (model 67051); a station for remelting and reconstituting mold pattern mixtures (model 64051) that comprises a Model 64502 autoclave and a Model 61551 apparatus for reconstituting pattern material; and a station for removing ceramic from cast blades (Model 67151). Design work has been suspended on the other eight stations. Lately, small and medium-sized investment foundries have become more commonplace, and SKBTL can design and prepare the documentation for the customized equipment used in these foundries. Figures 3.

Flexible Die-Casting Machines

927D0235A Moscow LITEYNOYE PROIZVODSTVO in Russian No 5, May 1992 pp 7-8

[Article by V. N. Voykin and V. L. Rudnik, Special Design Bureau of Casting Process Technology; UDC 621.74.043]

[Abstract] Technical specifications and performance characteristics are provided for three new flexible die-casting machines: the GPM711107, the GPM711108, and the GPM711109 (GPM - flexible manufacturing module). These standardized units are fully computer automated and capable of producing aluminum, zinc, and magnesium castings with exceptional mechanical properties, structural integrity, dimensional accuracy, and surface quality, even in castings with wall thicknesses of only 0.8 to 1 mm. The quality of these castings is attributed to the fully computer-automated process-control system and to the newly designed plunger mechanism used in these units. The plunger is a three-phase, hydraulically amplified, vertically-mounted, gas-driven mechanism. Casting pressure is smoothly adjusted by pumping ballast into one of the gas tanks. The clamping mechanism has sensors for automatically setting an unalterable clamping force and a device for automatically regulating the motion of the movable die plate and ejector plates. The hydraulic circuitry used to control the clamping mechanism is designed to prevent undesirable movable die plate motion. The die-lubrication and metal teeming devices are electromechanically driven and programmable. The casting stripper has a hydropneumatic drive and a vertical slide that allows it to place the finished casting on a conveyor or on the work table of a trimming press. All moving parts hazardous to shop personnel are fitted with protective covers of modern design. These machines have greater productivity than previous models and can be more quickly and easily set up for different casting operations. Tables 2.

Selecting Wear-Resistant Surfaced Metal for Operation Under Abrasive Wear Conditions

927D0241G Moscow SVAROCHNOYE PROIZVODSTVO in Russian No 5(691), May 92 pp 31-33

[Article by B.V. Danilchenko, Electric Welding Institute imeni Ye.O. Paton; UDC 621.791.92.042:669.018.25]

[Abstract] The shortcomings of the Cr/C ratio in the deposited layer for assessing the service properties of surfaced metal intended for operation under abrasive wear which does not take into account the structural features and phase composition of the deposited metal as well as the surfaced metal alloying with Mn, Ti, V, and other metals made it necessary to formulate a principally new approach to selecting the available surfacing materials for the specific operating conditions and developing new abrasive wear resistant materials. The problem is reduced to deriving an equation and developing on its basis charts which make it possible to establish the relationship between the surfaced metal content, structure, and phase composition on the one hand and the deposited metal wear resistance under abrasive wear on the other. The effect of the alloying elements on the structure and wear resistance of the deposited metal with and without boron is plotted. The resulting charts, together with existing notions of the abrasive wear resistance of various structural components of the surfacing materials—carbides, carboborides, borides, austenite, and martensite—make it possible to determine the most efficient materials analytically and solve the problem of assessing the suitability of available materials. Figures 1; references 8.

Properties of Thin-Film Emission Structures Based on Solid Solutions of $La_xY_{1-x}B_6$

927D0215G Kiev POROSHKOVAYA METALLURGIYA in Russian No 6, Jun 92 pp 97-101

[Article by A. M. Vasilyev, V. I. Bessaraba, Ye. M. Dudnik, A. V. Kovalev, and L. R. Shaginyan, Institute of Problems in Materials Science of the Ukrainian Academy of Sciences, Kiev; UDC 669.851/86:539.23]

[Abstract] The concentration of yttrium in a solid solution based on lanthanum hexaboride was varied to determine its effect on the structure and certain properties of film cathodes made from $La_xY_{1-x}B_6$ solid solution. Powders were made from the borothermic reduction of mixtures of lanthanum and yttrium oxides in titanium diboride crucibles in a 6.5×10^{-2} to 1.3×10^{-3}-Pa vacuum for 2 h at 1875 to 2000 K. The cathode films were made by electron beam evaporation of the powders with subsequent condensation onto pre-coated leikosapphire substrates in a 1.3×10^{-3}-Pa vacuum. The films, which were 4.0 to 5.0 μm thick, were annealed at temperatures equal to or 50 to 100 degrees higher than the deposition temperature [not indicated].

X-ray diffraction (DRON-2.0 diffractometer) and reflection electronography (EMR-100 electronograph) were used to control film-specimen phase composition. A direct-current diode circuit was used to study emission characteristics. The specimens were heated at 60-70 degrees/minute to 1073 K, then at 20-30 deg/min to 1623 K and held at this temperature for 20 to 30 min. Current strength as a function of cathode temperature was measured at temperatures between 1373 and 1623 K every 20 degrees. Thermal emission was also measured as the temperature decreased. This procedure was repeated several times. Thermoemittive films with an yttrium concentration of at least 30% have a relatively low output work value (φ = 2.19) and high emission current density (j = 0.53 A/sq cm) at a temperature about 400 K lower than LaB_6-based specimens made in the same way. Higher yttrium concentrations result in poorer thermoemissive characteristics, possibly due to the formation of yttrium boride phases. Figures 5, tables 2; references 3: Russian.

Certain Physical Properties of Zirconium-Matrix Composite Materials

927D0215F Kiev POROSHKOVAYA METALLURGIYA in Russian No 6, Jun 92 pp 93-97

[Article by L. R. Vishnyakov, V. P. Moroz, and P. I. Malko, Institute of Problems in Materials Science of the Ukrainian Academy of Sciences, Kiev; UDC 621.762: 669.296:621.763: [669.27+669.28:539.216]

[Abstract] Thermal conductivity, specific resistivity, and the coefficient of thermal expansion were studied at temperatures between 20 and 1000°C in zirconium-matrix composite materials reinforced with tungsten and molybdenum fibers and mesh. The material was made from iodide zirconium foil 100 μm thick reinforced with unidirectional fibers of MCh molybdenum or VA titanium 100 μm in diameter or with sink-stitched knit mesh 30 μm in diameter. The material was compacted into sheets by diffusion welding packets of alternating layers of the foil and reinforcing material in a vacuum. The fibers constituted 32% of specimen volume, and the mesh 13%. Electron discharge machining was used to cut test specimens 8 x 10 x 40 mm from the sheet in such a way that the fibers were aligned parallel or perpendicular to the specimen axis. The results of the study showed that thermal conductivity is higher in the zirconium composite than in pure zirconium, especially when the mesh reinforcement is used. At 1000°C, thermal conductivity was about twice as high for the composite as for the pure material. Electrical resistivity, however, was as much as 2-2.2 times lower for the composite specimens than for the pure zirconium specimens, regardless of the type or nature of reinforcement used. The coefficient of thermal expansion for the composite materials was somewhat lower than or comparable to the pure materials, varying from 4.4 to 4.9. Figures 3, tables 1; references 10: Russian.

Scaling Resistance of Binary Titanium and Chromium Carbides Made by Self-Propagating High-Temperature Synthesis

927D0215E Kiev POROSHKOVAYA METALLURGIYA in Russian No 6, Jun 92 pp 31-35

[Article by G. N. Komratov and V. M. Shkiro, Institute of Structural Macrokinetics of the Russian Academy of Sciences, Chernogolovka; UDC 546.261:620.193]

[Abstract] The oxidation kinetics of binary titanium-chromium carbides were studied. The carbides were synthesized in a laboratory self-propagating high-temperature synthesis reactor from PTM titanium and PKh1-S chromium powders and PM-15TS carbon black. The concentration of chromium carbide was varied from 5, 10, 15...45% (9 compositions in all, with a grain size of 80/40 μm). Two-gram powder specimens were oxidized in a muffle furnace at 600°C in atmospheric air. X-ray phase analysis of the oxidized specimens showed that the scaling resistance of binary Ti-Cr powders depends on the Ti/Cr ratio. Although specimens with a chromium carbide content of at least 35% had the highest resistance to scaling, none of the specimens studied were as resistant to scaling as pure chromium carbide. Initially, during the first 3 hours, oxidation obeys the parobolic law; after 3 hours, the process slows down considerably. The limiting stage of the oxidation process is the diffusion of reactants through the accumulating layer of scale. Figures 6, tables 1; references 10: 8 Russian, 2 Western.

Decarburization of Tungsten Carbide During the Electrolytic Application of Cobalt Coatings From Aqueous Solutions

927D0215C Kiev POROSHKOVAYA METALLURGIYA in Russian No 6, Jun 92 pp 20-23

[Article by Yu. M. Korolev, Yu. M. Polukarov, and V. M. Zanozin; the All-Union Scientific Research Institute of Refractory Metals and Hard Alloys, Moscow, and the Institute of Physical Chemistry of the Russian Academy of Sciences, Moscow; UDC 621/762.001:541.13]

[Abstract] A study of the quantitative parameters of an electrochemical process for applying cobalt plating to tungsten carbide has shown that the decarburization that occurs during this process is caused by a reaction between the carbide and adsorbed atomic hydrogen, rather than by the washing away of free carbon or by anodic corrosion, has had previously been hypothesized. The chemical formula representing the decarburization process is presented and discussed. An analysis of the effect of electrolytic process conditions on decarburization showed that higher carbon losses are associated with lower powder dispersivities and greater partial current densities. Thus, by lowering current density and increasing the degree to which the powder is dispersed, carbon losses can be minimized, making it possible to produce cobalt-coated tungsten carbide powders with a carbon content of at least 0.1%. Figures 3, tables 1; references 5: Russian.

Compaction of Spontaneous High-Temperature Synthesis Materials

927D0215B Kiev POROSHKOVAYA METALLURGIYA in Russian No 6, Jun 92 pp 14-19

[Article by K. L. Yepishin, A. N. Pityulin, and A. G. Merzhanov, Institute of Structural Macrokinetics of the Russian Academy of Sciences, Chernogolovka; UDC 546]

[Abstract] The process whereby combustion products are compacted was studied using Zr-C, Ta-C, Ti-B-Cu, and Ti-Cr-C-Ni systems as examples. The charges were prepared from PTsrK-1, PTsrK-3, and PTsrN-V zirconium powders, PTM titanium powder, tantalum, Pkh-1S chromium

powder, PNE-1 nickel powder, and PMA copper powder, PM-15TS carbon black, and amorphous brown boron powder. The powders were mixed in steel ball mills in air or in industrial ethyl alcohol. The charges were dried in a ShSVA-2.4-type drier and compacted on a manually operated hydraulic press into tablets 50-70 mm in diameter and 20-30 mm long. The specimens were compacted by self-propagating high-temperature synthesis on a D1932 press in thermally insulated closed steel dies. The press was equipped with an automated unit for setting compacting conditions. Chemical and x-ray phase analyses were used to determine the concentration of basic components and impurities in the materials. Total, apparent, and closed porosities and porosity prior to reaching the necessary pressure were determined experimentally using the "kerosene" sample method, which combines hydrostatic weighing and impregnation of the specimen with a liquid such as kerosene or isobutyl alcohol. It was found that the compaction process goes through a sliding stage, a plastic deformation stage, and a stage during which the pores are filled by diffusion. The nature of compaction depends on the composition of the reactive mixture and on compacting conditions. The presence of a liquid phase that adequately lubricates the refractory component is a key factor in this regard. Figures 5, tables 1; references 14: Russian.

Sintering Simple Metal Oxides With Variable Valency

927D0215A Kiev POROSHKOVAYA METALLURGIYA in Russian No 6, Jun 92 pp 7-10

[Article by Yu. I. Boyko, Yu. I. Klinchuk, and V. P. Sukhomlin, University of Kharkhov; UDC 621.762]

[Abstract] The process of sintering copper oxides in oxygen was studied to determine: 1) whether the process of sintering simple metal oxides actually occurs through the mechanism of diffusion; 2) whether it is the diffusion of the metal or the oxygen ion that is the limiting factor in substance transfer during sintering; and 3) how changes in oxygen pressure affect the diffusion mobility of the oxide-forming elements. Cylindrical copper oxide compacts 3 mm long and 10 mm in diameter were formed from a spheroidized powder with an average dispersity of app. 20 μm. Compacting pressure was 3×10^2 MPa. Sintering temperature was 750-1050°C, with an isothermal holding period of 1 to 10 hours. Dilatometric measurements and a KM-8 cathetometer were used to study the specimens during the sintering process. It was found that sintering at these temperatures does occur through the diffusion mechanism and that the rate of substance transfer is limited by the diffusion of oxygen and is directly dependent on the process of dissociation. Active dissociation begins when the oxygen in the lattice of the original oxide reaches maximum solubility and is given off in a gaseous phase, and when an excess concentration of anionic vacancies appears, both of which together promote an increase in sintering speed. It is concluded that these phenomena are typical for all simple metal oxides with variable valency and need to be taken into account when developing production processes for ceramics based on these types of compounds. Figures 2; references 9: Russian.

Effect of Plasma Chemical Vapor Deposition on Wear-Resistance of Medium- and Low-Carbon Steels

927D0194D Minsk TRENIYE I IZNOS in Russian Vol 13, No 3, May-Jun 92 pp 533-535

[Article by L. A. Timofeyeva, S. A. Katrich, and L. A. Solntsev, Kharkov Vehicular Roadway Institute; UDC 663.131.4.663.69]

[Abstract] Specimens of 40Kh and 18KhGT steel were studied to determine the effect of plasma CVD coatings on the friction moment during dry friction and friction with boundary lubrication. The specimens were pre-cleaned for 3 min. with a beam of titanium ions at 1000 V and a residual gas pressure of 10^{-5} mm Hg in the chamber. A titanium nitride coating was formed on the specimens by plasma CVD in an atmosphere of titanium vapors and nitrogen at a pressure of 4 to 5×10^{-3} mm Hg. Deposition time was 20 min. Coating thickness was 5 μm. The specimens underwent block and ring testing with a steel disk on a modified MI-1-type friction tester at a pressure of 8.4 MPa and a disk rotational frequency of 16.6 s^{-1}. During testing without a lubricant, the friction moment was initially 2 to 2.5 times higher for the coated than for uncoated specimens, but as wearing-in progressed, the friction moment for the coated specimens uniformly decreased until it was 20% lower than the friction moment for the uncoated specimens. Under boundary lubrication conditions, the friction moment was more than 5 times lower for the coated than for the uncoated specimens. The low friction moment for the coated surfaces was attributed to their high adsorptivity, which was activated by the coating process. This adsorptivity greatly enhances the effectiveness of a lubricant. During the course of the testing, it was found that a low friction moment could be achieved by coating just one of the parts. The coatings were field tested by applying them to the axle and bushing assembly of a VPR-1200 railway repair machine. The coatings were applied in the same manner as those applied during laboratory testing. The field tests showed that the coated parts had a wear resistance 2.5 to 3 times higher than that of uncoated parts. Figures 1, tables 1; references 2: Russian.

Friction and Wear Properties of Self-Forming Coatings

927D0194C Minsk TRENIYE I IZNOS in Russian Vol 13, No 3, May-Jun 92 pp 528-532

[Article by V. D. Zozulya, A. R. Kachin, and V. I. Yukhvid, Institute of Structural Macrokinetics of the USSR Academy of Sciences, Moscow; UDC 621.891:621.762:621.793]

[Abstract] The effects of structural features and load conditions on friction and wear properties were studied in coatings applied by the combustion of charges containing chromium, titanium, carbon, boron, and iron on the worn end surfaces of St3 steel specimens 5 x 5 x 17 mm. The resurfaced specimens underwent friction and wear tests in a testing machine equipped with a roller-type shaft 40 mm in diameter made from steel 45 and heat-treated to a hardness of 49-51 HRC. Friction test speed was 1 m/s, load ranged from 1-20 MPa, and the capillary lubricant was Industrial-20 oil. Wear was measured and recorded by an inductive sensor coupled with a plotting device, which

made it possible to graph the wear rate and the friction moment without stopping the friction tester. Friction tests were also performed on uncoated St3 steel specimens and on specimens of BrOF-10-1 bronze, which is one of the best low-friction materials available. The test results showed that wear resistance was appreciably higher for the test pieces resurfaced with the self-forming coatings. X-ray spectroscopy revealed that, at the coating/steel interface, coating structure consisted of solutions of titanium, chromium, carbon, and boron in iron. The structure of the coating layer directly exposed to wear had a columnar structure of carbides evenly distributed throughout the tough solution matrix, parallel to the vertical load on the friction system. The presence of a uniform transitional diffusion zone at the coating/steel surface interface strengthens the bond between the coating and the substrate and prevents frictional heat from causing the coating to separate from the metal surface due to different thermal expansion coefficients. The tough and elastic intermediate layers of the coating act as a buffer zone that dampens and disperses the shock from sliding friction. The structure of the friction layer is capable of distributing the load uniformly throughout the matrix and of resisting wear caused by tangential frictional forces. Figures 5; references 6: Russian.

Abrasive Wear of Steels Hardened With Different Combinations of Shock-Wave and Thermal Laser Processes

927D0194B Minsk TRENIYE I IZNOS in Russian Vol 13, No 3, May- Jun 92 pp 524-527

[Article by P. Yu. Kikin, A. I. Pchelintsev, and Ye. Ye. Rusin, Institute of Machine Design imeni A. A. Blagonravov of the USSR Academy of Sciences, Gorkov Affiliate; UDC 621.891:621.375]

[Abstract] Abrasive wear was tested on carbon steels 20, 45, and U8, which were hardened either by a combination of laser hardening followed by shock-wave hardening or by a combination of shock-wave hardening followed by laser hardening and another shock- wave treatment. For comparative purposes, the steel specimens were also laser-hardened only. Laser hardening was carried out with a pulsed laser operating on YAG:Nd^{3+} with a power density of 40,000 W/sq cm. Shock-hardening was effected with a ruby laser operating with a modulated energy factor with typical parameters being: impulse energy E = 1.5 J, and t = $(20...25)10^{-9}$ S. The shape and amplitude of the shock wave were measured with a Michaelson laser interferometer. The Brinell-Havort method was used to measure hardness. The data showed that, for all three steels, the greatest increase in hardness was attained when laser hardening was sandwiched in between shock-wave hardening. During the first shock-wave treatment, a defective structure is formed on the surface layer of the steel, thereby making the conditions for phase transformation during the laser process highly favorable. Subsequent re-treatment with the shock-wave process decreases the concentration of residual austenite in the structure of the hardened steel, transforming it into deformation martensite. Thus, the wear resistance of steel treated in this manner can be increased by as much as two-fold over that of conventionally laser-hardened steel. Figures 3, tables 1; references 3: Russian.

Effect of Radial-Shift Rolling on the Quality of Semifinished Titanium Alloy Products

927D0190L Moscow TSVETNYYE METALLY in Russian No 5, May 92 pp 56-57

[Artick by Ye. A. Kharitonov, I. N. Potapov, I. Z. Volshonok, V. S. Dushin, A. I. Zhuravlev, V. M. Arzhakov, Moscow Institute of Steel and Alloys, All-Union Institute of Aviation Materials, VSMPO; UDC 621.74:669.295]

[Abstract] Production of high-quality titanium alloy rods with a controlled macrostructure by the method of radial-shift rolling could significantly facilitate the process of making stampings for use in critical assemblies. To determine the possibility of making such products, studies were first conducted to examine the effect of radial-shift rolling on the forming of the structure of rods rolled on a radial-shift mill, and to select parameters for rolling in industrial-scale production. In the second stage, stampings made from 135 mm diameter rods rolled according to the selected parameters were examined. Analyses of the macrostructure of the rolled rods indicated that radial-shift rolling produces a uniform recrystallized structure in titanium alloy rods, and the process of obtaining a controlled macrostructure can be regulated by altering the deformation and using intermediate heating. Subsequently, the technique for manufacturing disks and blades from rods rolled on a radial-shift mill was tested in industrial conditions. The macrostructure of stampings manufactured by this simplified technique was found to have somewhat more discontinuity than counterparts made by the conventional method, but overall their mechanical properties were practically in the same range and satisfied technical standards.

Effect of Heat Treatment on Uniform Elongation of Medium Carbon Steel

927D0225A Moscow METALLOVEDENIYE I TERMICHESKAYA OBRABOTKA METALLOV in Russian No 7, Jul 92 pp 6-7

[Article by A. A. Azarkevich, A. A. Pashchenko, and T. A. Yevtukhova, Ukrainian Research Institute of Metallurgy; UDC 669.14.018.298.3:621.785.796]

[Abstract] The possibility of replacing 35KhGSA medium carbon steel with 35GSR steel for making connectors for attaching the paddles to chains in flight conveyors was investigated. Connectors made of 35KhGSA steel do not meet industry standards for breaking load and elongation. To determine whether 35GSR steel is a suitable replacement, it was of interest to investigate how uniform elongation of the steel depends on its heat treatment conditions and strength properties. Cylindrical specimens were made out of heat-treated billets of 35GSR steel with different carbon contents and they were tested on a tension machine. Together with relative elongation and reduction in area, uniform elongation was determined according to tension plots and, for comparison, according to the diameter of specimens after breaking. The character of the dependence of strength and plastic properties on the tempering temperature for specimens with different carbon contents was found to be identical. When tempering temperature is increased from 300 to 550 degrees C, strength characteristics decrease monotonically. Analysis of the effect of heat treatment conditions on uniform elongation of 35GSR steel showed that the tempering temperature of connectors can be decreased to 300-350 degrees C, with an increase in their strength properties at values of uniform elongation which meet industry standards for residual deformation.

Oxidation of Pipe During Combined Furnace and Induction Heating

927D0225B Moscow METALLOVEDENIYE I TERMICHESKAYA OBRABOTKA METALLOV in Russian No 7, Jul 92 pp 8-9

[Article by A. A. Zgura, O. T. Nikolskaya, T. V. Ivanova, and I. S. Stefanskiy, All-Union Research Institute of Pipes, Dnepropetrovsk; UDC 621.774:621.78.012]

[Abstact] The degree of oxidation of carbon steel pipe in the combined furnace and induction heating method was investigated with furnace heating first followed by induction heating, and vice versa. The degree of oxidation was also determined for both furnace and induction heating separately. It was found that in the combined method with furnace heating first followed by induction heating, with the pipe heated to 400-600 degrees C in the furnace, the degree of oxidation of the metal is minimal (0.5-0.55% of the weight of the pipe). Furnace heating above 600 degrees

followed by induction heating increases oxidation of the metal to 0.9%. With induction heating alone, oxidation of the metal is practically identical to oxidation in combined heating with the furnace first followed by induction heating, which demonstrates the advantage of the combined method (less electricity consumed than in straight induction heating). Combined heating with induction first followed by furnace heating has the highest degree of oxidation, and this method is recommended only for installations that have a shielding gas atmosphere.

Electron Beam Treatment of Bearing Steels

927D0225C Moscow METALLOVEDENIYE I TERMICHESKAYA OBRABOTKA METALLOV in Russian No 7, Jul 92 pp 13-17

[Article by A. A. Shulga, Taganrog Radiotechnical Institute; UDC 621.9.048.7:669.018.24]

[Abstract] The effect of the initial state of the metal and of electron beam treatment parameters on formation of a hardened layer in the bearing steels ShKh15 and ShKh15SG and the carburized steel 15G1 was investigated. Specimens of these steels underwent different heat treatments prior to electron beam treatment. The initial structure of preannealed steels ShKh15 and ShKh15SG was granular pearlite, and after undergoing oil hardening from 840 degrees C and tempering at 150 degrees C for 2 hours, the structure was fine-crystalline martensite, retained austenite (up to 5%), and finely dispersed carbides. Specimens of 15G1 underwent gas carburizing, oil hardening and tempering at 160 degrees C for 2 hours. The thickness of the carburized layer was about 1.5 mm. Electron beam treatment was done with a ribbon beam 0.5-2.0 mm thick and 40 mm wide and having a power of 1,000-50,000 W per square centimeter. The beam's rate of movement was 0.5-4.0 cm/s. Microstructural analysis of the treated specimens revealed both general regularities and peculiarities of the formation of the structure and substructure of the steels. After electron beam treatment, a hardened layer with martensitic-austenitic structure was formed on the surface of all the specimens, and their structural peculiarities were conditioned by the high rates and short duration of heating. With this treatment fusion of the surface takes place with formation of a hardened zone from the liquid phase. In all the specimens, high-temperature heating led to dissolving of carbides in this zone at rates of beam movement up to 2.5 cm/s. At higher rates of movement in ShKh15 and ShKh15SG steels with an initial pearlite structure, the largest carbides to not manage to dissolve. Structural peculiarities of the hardened layers and deeper layers of the examined specimens depending on different initial states of the metal and different electron beam parameters are presented, and their significance for the performance properties of the treated steels in bearings is discussed. Results of tests of bearings made with electron beam treated steels are presented. Principal conclusions drawn from the tests are:

1. The structure and properties of electron beam treated bearing steels depend largely on their initial structure and the composition of the carbide phase. This type of treatment is best used for hardening steel with an initial finely dispersed structure. Maximum hardness and density of dislocations are found in the zone hardened from the solid state without full dissolving of carbides.

2. In comparison with laser treatment, electron beam treatment makes it possible to avoid decarburization of the surface layer and to obtain a more uniform structure in the beam's direction of movement as well as a thicker hardened layer.

3. To obtain bearing steels with high contact durability, it is necessary to perform electron beam treatment without the surface fusing and under conditions where carbides do not dissolve completely and a hardened layer forms.

4. Contact durability of roller bearing surfaces after electron beam treatment depends on the thickness of the secondary hardened zone. Increasing the service life of bearing surfaces is possible only if the thickness of the hardened layer exceeds by at least 50% the depth at which the zone of maximum tangential stresses from rolling lies.

Effect of the Content of Alloying Elements in Different Grades of Alloy KhN65KVMYuTB on Its High-Temperature Strength

927D0225E Moscow METALLOVEDENIYE I TERMICHESKAYA OBRABOTKA METALLOV in Russian No 7, Jul 92 pp 29-31

[Article by M. A. Filatova, V. S. Sudakov, and I. V. Kabanov, Scientific and Production Association of the Central Research Institute of Machinery Manufacturing Technology, and the "Elektrostal" Plant; UDC 669.14.018.44:620.17]

[Abstract] The nickel-base alloy KhN65KVMYuTB was investigated to determine what effect the content of aluminum and titanium in different grades of it has on its high-temperature strength. In the medium grade of the alloy, the aluminum content is 1.8% and the titanium content is 1.7%, and in its high grade the percentages of these elements are 2.4 and 2.6, respectively. Thus, the combined content of Al and Ti in the alloy's chemical composition is in the range 3-5%. As a rule, in nickel alloy production the furnace charge is calculated using the mean content of each alloying element. Results of the investigation showed that the higher level of Al and Ti content (approximately 2.5% each) increases the alloy's long- and short-term strength as well as fatigue resistance by as much as 20% in comparison with the medium grade level, while properties that determine its workability under hot pressure treatment remain at a satisfactory level.

Deformation Waves Near Nonmetallic Inclusions in Explosive Working of Metals

927D0225F Moscow METALLOVEDENIYE I TERMICHESKAYA OBRABOTKA METALLOV in Russian No 7, Jul 92 pp 32-33

[Article by S. I. Gubenko, Dnepropetrovsk Metallurgical Institute; UDC 669.14.018.298:621.9.044]

[Abstract] The effect of nonmetallic inclusions as concentrators of deformation in steel undergoing explosive working was investigated. Specimens of two brands of tempered steels were subjected to dynamic loading through the transmitting medium of a propelled plate. The microstructure and substructure of the steels near non-deforming inclusions of silicon and aluminum oxides were examined.

The investigations revealed that, near nonmetallic inclusions, there occur relaxation processes of a translational-rotational type having a wave character. These processes lead to the formation of complexly deformed structures in the relaxation waves. In zones of plastic relaxation the microhardness is higher than in the matrix away from inclusions. When there are several waves the microhardness of the relaxation zone is heterogeneous. Away from an Al_2O_3 inclusion 30 micrometers in size the microhardness was found to be 154 H, and in the first and second relaxation waves it was 164 and 178 H, respectively, while directly near the inclusion in the third relaxation wave it was 189 H.

Niobium's Effect on the Structure of Chromium Ferritic Steel

927D0225G Moscow METALLOVEDENIYE I TERMICHESKAYA OBRABOTKA METALLOV in Russian No 7, Jul 92 pp 35-38

[Article by G. A. Burakova, Ye. K. Koval, and M. I. Tarasyev, Dnepropetrovsk Metallurgical Institute; UDC 669.15'26'293-194]

[Abstract] The possibility of increasing the corrosion resistance of vacuum heat-treated steel used in pipes by alloying with niobium was investigated. Pipes made of 01Kh25 chromium ferritic steel which are vacuum heat-treated have good resistance to intercrystalline corrosion, but welds made in them are subject to this corrosion. Steel of this brand was melted in an induction furnace and cast into 10-kg round ingots. After forging into sheet 8-10 mm thick, specimens were vacuum treated at 1300 degrees C for 40 hours and then rolled warm to a thickness of 3 mm. Specimens with different Nb contents (0.23, 0.46 and 0.83%) were tested. The tests produced the following conclusions:

1. In 01Kh25 steel alloyed with 0.23, 0.46 and 0.83% Nb, an excess mu-phase is formed which embrittles bended specimens in tests for intercrystalline corrosion. Grain boundaries remain clean and are not subject to corrosion failure. The steel's resistance to overall corrosion is increased by 50% when alloyed with a minimum of 0.46% Nb.

2. The presence of small particles of the mu-phase in Nb-alloyed 01Kh25 steel does not have a detrimental effect on its warm-rolling deformability.

3. The optimum Nb content for ensuring high corrosion resistance and obtaining an optimum structure for steel which undergoes vacuum heat treatment is 0.4%.

Nature of the Internal Friction Peak in Beryllium at 100-200 Degrees C

927D0225H Moscow METALLOVEDENIYE I TERMICHESKAYA OBRABOTKA METALLOV in Russian No 7, Jul 92 pp 38-40

[Article by G. F. Tikhinskiy, I. I. Papirov, V. M. Arzhavitin, B. I. Shapoval, and G. Ye. Pletenetskiy, Kharkov Physico-Technical Institute; UDC 539.67:669.725]

[Abstract] In a number of metals whose crystal lattice has a hexagonal close-packed structure (e.g. Zr, Zn, Be), internal friction peaks are observed at comparatively low temperatures (up to 300 degrees C). To understand the nature of this kind of peak in beryllium, the relationship of its characteristics to the metal's purity, its structural state, and the rate of heating of specimens and other heat treatment parameters was investigated. Earlier investigations attributed the appearance of the internal friction peak to interaction of interstitial atoms with moving dislocations. The present investigation did not exclude the effect of impurities but considered it to be a secondary factor, because in beryllium at 200 degrees C, substantial changes in the distribution of impurities cannot take place due to their low diffusion mobility, and thus impurities should not by themselves cause internal friction anomalies. Studies of the asymmetrical internal friction peak were made in the temperature range 20-300 degrees C using specimens of polycrystalline beryllium with different levels of purity. The results demonstrated that in the temperature range 100-200 degrees C, internal thermal stresses are the main cause of the appearance of the internal friction peak in beryllium. Impurities have only an indirect influence, acting on processes of the origin and relaxation of stresses.

Plasma Technologies in Building Practices

927D0240B Moscow SVAROCHNOYE PROIZVODSTVO in Russian No 4(690), Apr 92 pp 5-7

[Article by G.A. Zadvornev, Togliatti Polytechnic Institute; UDC 621.791.755:691]

[Abstract] The new requirements being imposed by the implementation of plasma technologies—particularly plasma welding—on low-temperature plasma generators, particularly increasing their original life and overhaul period while using air as the plasma-forming gas and power supply sources with a ≤520 V no-load voltage, are discussed. Schematic diagrams of plasma generators and the voltage-current characteristics of plasma generators with a diaphragm and with gas delivery through the anode as well as the volt-ampere characteristics under various gas delivery conditions are cited. Various types and connection methods of diaphragms—interelectrode inserts—as well as gas delivery methods are examined in order to optimize the plasma generator designs. A study of the effect of gas delivery variations reveals that the optimum design calls for delivering the plasma-forming gas only between the anode diaphragm and the anode. Plasma cutting methods used for nonmetallic materials (e.g., by Union Carbide), rocks, and metals are investigated and the use of plasma arc torches with a >10,000°C temperature is discussed. New low-temperature plasma applications for making new popular materials, e.g., metal-concrete composites, are outlined. The energy characteristics of plasma technologies, especially in melting metals, are analyzed. From the economic viewpoint, the implementation of plasma technologies in construction practices is quite profitable. In Togliatti alone, the economic impact from their implementation reached 120,000 rubles in 1990 and 600,000 in 1991. Figures 1; references 5.

Three-Phase Arc Surfacing of Aluminum Alloy Products

927D0240C Moscow SVAROCHNOYE PROIZVODSTVO in Russian No 4(690), Apr 92 pp 7-8

[Article by V.V. Yeltsov, V.F. Matyagin, Togliatti Polytechnic Institute; UDC 621.791.927.5:537.63:669.71]

[Abstract] The problem associated with restoring aluminum alloy parts by arc deposition due to a decrease in the arc's thermal impact on the surfaced metal prompted the development of a new surfacing method for restoring aluminum alloy parts which makes it possible to overcome existing difficulties due to using the burning characteristics of a three-phase arc in argon and its effect on the welded metal. In essence, the filler wire is connected to one of the phases of the UDGT current source in place of the product. Using this method, an experiment is conducted to surface an AD0 alloy plate with an AMg61 wire and the surfacing process is investigated with and without connecting the filler wire to the "product" phase. The temperature distribution of the proposed and traditional surfacing methods and the welding strain under the proposed and traditional methods are plotted. The three-phase arc burns simultaneously on the product and on the filler wire, ensuring a good cathode purification of the base and filler material and facilitating their intense melting. The method makes it possible to decrease the thermal impact of the arc and increase the deposition intensity. Figures 5; references 4.

Aluminum Alloy Product Surfacing Using Molten Filler

927D0240D Moscow SVAROCHNOYE PROIZVODSTVO in Russian No 4(690), Apr 92 pp 8-9

[Article by Z.A. Shamugiya, Togliatti Polytechnic Institute; UDC 621.791.927.5:537.63.669.71]

[Abstract] The difficulty of restoring aluminum alloy parts with a large surface and the overheating of the heat affected area (ZTV) which may lead to a burnout of some alloying elements as well as the negative impact of multiple overheating characterizing traditional surfacing methods are discussed and it is suggested that a filler metal melted beforehand (RPM) be used for surfacing parts with a flat surface. Simultaneous surface activation by the heated tool immersed in a molten filler metal makes it possible to deposit it to a rather large surface and conduct the process at a base metal melting point. The main parameters of the process are investigated and the findings are presented; a method to restore parts from casting aluminum alloys is developed on the basis of these results. The restored part rejection ratio does not exceed 5-10%, i.e., is considerably lower than that of traditional procedures. Thus, mechanical activation of the surface with simultaneous molten metal deposition makes it possible to produce a good adhesion over a large area. The surface activation time, surfacing rate, and filler metal temperature are the main parameters affecting the adhesion quality. Figures 2; references 2.

On Deterministic Representation of Soldered Copper Alloy Unit Corrosion in Sea Water

927D0240E Moscow SVAROCHNOYE PROIZVODSTVO in Russian No 4(690), Apr 92 pp 14-15

[Article by R.S. Luchkin, Togliatti Polytechnic Institute; UDC 621.791.3:658.562]

[Abstract] The large number of electrochemical failure processes and the factors which have a simultaneous and often opposite effect on the soldered joint and unit corrosion rate and complicate analytical estimates of the state of joints and units under the specific operating conditions prompted an attempt to represent the corrosion of soldered units and joints as random processes or deterministic time functions. The selection of the specific group of failure process models is determined by the purpose of each study and the need to take into account various factors in the behavior of the electrochemical systems under study (EKhS) in the time domain. The behavior of transient processes under a potentiostatic disturbance of the welded joint in calm sea water is plotted; the time variations of the mathematical expectation and unbiased variance estimates are summarized; an analysis shows that the principal statistical parameters are not constant in time. The results demonstrate that the deterministic representation at fixed initial corrosion conditions is a particular case of a stochastic approach to the analysis of failure processes while the effect of the initial failure parameters can be ignored and considered to be deterministic only under a steady-state corrosion process. Figures 1; tables 1; references 7.

Characteristics of Coat Application Practices in Vacuum Using Electric Arc Evaporators

927D0240A Moscow SVAROCHNOYE PROIZVODSTVO in Russian No 4(690), Apr 92 pp 4-5

[Article by Ye.Ya. Prokoshenkov, S.L. Kudryashov, O.N. Neretin, Togliatti Polytechnic Institute; UDC 621.793.7.01]

[Abstract] Vacuum application of protective coats on the wear surfaces of parts and tools which improve their performance, particularly ion plasma deposition methods using stationary electric-arc consumable-cathode erosion plasma accelerators are considered and a schematic diagram of an electric arc plasma source of ionized substance with self-stabilization and magnetic field confinement of the cathode spot is cited. The dependence of the mass variation of a slab from steel 10Kh18N10T on the negative base potential in a vacuum is plotted. The principal advantages of the method is its high degree of interacting component activity and the enhancement of the topochemical reactions on the base surface during the coat condensation which ensure a high quality and good physical and mechanical properties of the coat. The device changes the plasma current energy due to its origin, phase composition, and kinetic factor thus making it possible to control the temperature conditions, nucleation processes, coat development kinetics, and the coat growth mechanism which determine its homogeneity and characteristics. The deposition procedure and the use of quality assessment criteria designed for it improve the tool resistance and lead to a gain of 32,000 rubles at the AvtoVAZ production association alone. Figures 2; references 2.

Making Stamped-Welded Clutch Plates From Steel 65G

927D0238G Moscow SVAROCHNOYE PROIZVODSTVO in Russian No 2(688), Feb 92 pp 26-28

[Article by V.S. Lysov, A.P. Suvorov, S.A. Yevsyukov, Cheboksary Industrial Truck Plant and Moscow State Engineering University imeni N.E. Bauman; UDC 621.791.754:631.372]

[Abstract] The high labor intensity of punching, machining, or cutting friction plates for various machines and the shortcomings of known welding methods prompted an investigation of the friction plate weld metal strength after hot stamping and its operating reliability in the gear box of a T-330 industrial truck. The effect of various welded joint shapes on the weld strength is examined in order to determine its strength after CO_2 welding with an Sv-08G2S wire. To this end, C7, C12, and C8 joints are made from steel 65G pursuant to GOST 14771-80; the welded joint quality is assessed by the absence of cracks revealed both visually and metallographically after 3 days, the metal structure and hardness in the welded joint area, and the welded joint metal ductility determined by the bend angle at fracture. The weld, base metal, and heat affected area properties are summarized and the structure and macrostructure of the welded joints are shown. An analysis of the findings demonstrates that the use of the C7 welded joint ensures a stable joint quality and the necessary performance properties during welding and hot stamping; the clutch plate blanks made by CO_2 arc welding of cylindrical billets with subsequent hot stamping ensure the necessary clutch plate properties. A pilot batch of 700 stamped-and-welded clutch plates was installed in gear boxes of the T-330 tractors and is currently undergoing commercial tests at the Production Association of the Cheboksary Industrial Truck Plant. Figures 3; tables 1; references 2.

Versatile Lab Plasma Unit

927D0238F Moscow SVAROCHNOYE PROIZVODSTVO in Russian No 2(688), Feb 92 pp 24-25

[Article by T.A. Gordiyenko, L.N. Sokolov, Central Scientific Research Institute of Ferrous Metallurgy; UDC 621.791.755.03-52]

[Abstract] A versatile lab unit intended for diverse high-temperature material treatments (at up to 5,000K), e.g., coat deposition, soldering, and other processes requiring heating, is described. An indirect-action plasma generator is used as the heating source; consequently, both conducting and insulating materials can be treated. A schematic diagram of the unit is cited and its operating principle is explained. An upgraded APR-402 air-cooled unit is used as the source. The plasma unit specifications are summarized and the power characteristic at a 0.95 efficiency (KPD) and the voltage-current characteristic of the APR-402 source at a 3 g/s nitrogen rate through the plasma generator are plotted. The interelectrode insert (MES) and the cathode unit are water cooled. The unit can also be used for examining the physical and chemical characteristics of the plasma arc discharge and mass transfer between the gaseous and metallic phases. The unit has a maximum installed capacity of 120 kVA. Figures 2; tables 1.

Welding Arc Igniter-Stabilizer

927D0238E Moscow SVAROCHNOYE PROIZVODSTVO in Russian No 2(688), Feb 92 p 24

[Article by A.V. Granovskiy, P.A. Gavrish, Kramatorsk Industrial Institute; UDC 621.791.753.9.93]

[Abstract] A welding arc exciter-stabilizer developed at the Department of Welding of the Kramatorsk Industrial Institute is described. It ensures a constant igniting pulse energy regardless of its phase and the possibility of controlling the pulse application phase independently at the moments of direct and reverse welding voltage polarity and has a low power demand of 60 W which favorably distinguishes it from similar commercial devices. The design and operating principle of the igniter-stabilizer are outlined and its electrical circuit diagram is cited. The device is reliable and makes it possible to weld Al and its alloys in argon by alternating current using both DC and AC electrodes. The device was tested with STSh-500, TSM-250, and TD-401 transformers. Figures 1.

Effect of Modifying Agents on Properties of Welded Joints of AMg6 Alloy

927D0238D Moscow SVAROCHNOYE PROIZVODSTVO in Russian No 2(688), Feb 92 pp 12-14

[Article by O.M. Novikov, V.O. Tokarev, O.Ye. Ostrovskiy, A.V. Gudkov, E.P. Radko, Scientific Research Institute of Mechanical Engineering Technology and Geopribortsvetmet Pilot Plant; UDC 621.791.01.052:539.4:669.71]

[Abstract] Cracks—the most common and dangerous defects which develop during the fusion welding of aluminum alloys—and the principal methods of eliminating them, e.g., metallurgical and physical, are discussed and it is noted that the metallurgical method, i.e., modifying the chemical composition of the weldpool and selecting the optimum thermal heating and cooling cycle in the welded metal, is the most promising. Thus, B, Zr, and Ti which possess the necessary range of modifying properties are tested in automatic welding of the AMg6 alloy. The chemical composition of the tested filler metals is listed. To examine the effect of modifying agents on the properties of the AMg6 alloy joints, slabs are joined by automatic argon arc welding using tungsten electrodes in a special welding bench with pneumatic clamps; the cracking tendency is examined in cross-pieces welded for this purpose. An analysis of 11 samples shows that the modifying agents do not affect the welded joint strength while the weld metal ductility and bend angle change, depending on the amount and type of modifying agents. An addition of 0.2 to 0.4% Bi to the filler wire increases the corrosion resistance; as a result, Bi-bearing wire is recommended for use in parts operating in especially corrosive media. The use of filler materials alloyed with Ti+B or Ti+Zr is recommended for decreasing the tendency to cracking. Figures 2; tables 3; references 3.

New Method and Equipment for Soldering Large Electric Machine Squirrel Cage Rotor Windings

927D0238C Moscow SVAROCHNOYE PROIZVODSTVO in Russian No 2(688), Feb 92 pp 5-7

[Article by M.M. Chernomorskiy, A.P. Korsakov, S.T. Poplaukhin, AP of Sibelektrotyazhmash Scientific Research Institute, Novosibirsk; UDC 621.791.3.03:621.313.131-17]

[Abstract] The difficulties of soldering the windings of squirrel cage rotors of large electric machines with round rods, especially the high labor outlays and poor soldered joint quality as well as a high level of residual mechanical stresses which lowers the operational reliability and durability of the windings, prompted the Sibelektrotyazhmash Scientific Research Institute to develop and the ELSIB enterprise to implement a new method and equipment for soldering squirrel cage rotors of large electric machines and design new ring fabrication processes. As a result of the new processes, the rod holes in the rings have the same cross section shape as the rods and have an optimum size for soldering with the necessary clearance; the dimensional accuracy of the holes is also quite high. The quality, work safety, labor intensity, Cu outlays, and electric power consumption of four hole-making methods—cold extrusion from a tube blank, by plasma cutting from rolled sheets and machining, by spin casting and machining, and by forging from a rod—are summarized. The soldering unit specifications are listed. The new methods make it possible to manufacture equipment for soldering rotors with a ring diameter of up to 1,000 mm weighing up to 200 kg. The development has a total economic impact of over 2 million rubles. Licenses for the equipment and methods are available on a contractual basis. Figures 3; tables 2.

Electron Beam Welding of Aluminum Nitride-Based Ceramics With Metals

927D0238B Moscow SVAROCHNOYE PROIZVODSTVO in Russian No 2(688), Feb 92 pp 4-5

[Article by M.P. Maloletov, V.A. Kazakov, O.N. Kudryashov, Tekhnomash Scientific Production Association; UDC 621.791.947.72:666.3.037.5]

[Abstract] The shortcomings of traditional methods, e.g., soldering and diffusion welding, for fully taking advantage of the properties of structural materials in metal-and-ceramics joints are outlined and it is speculated that electron beam welding of metals and ceramics is capable of realizing the properties of the metal/ceramic unit materials; this prompted an experimental investigation of electron beam welding of aluminum nitride with aluminum and copper. The process is conducted after a certain preheating since during fusion welding of ceramics and metals, the former may fail due to a thermal shock. The physical and chemical interactions of the process are examined in order to select the optimum welding metals and the materials' weldability is analyzed. A metallographic study reveals no pore, crack, and looseness-type defects in the ceramics. The method is used for making the contact surfaces on an aluminum nitride base. The resulting joint's shear strength is high and reaches 200 MPa. Figures 2; references 3.

Pressure Welding of Dielectrics Through Electrically Exploded Layers

927D0238A Moscow SVAROCHNOYE PROIZVODSTVO in Russian No 2(688), Feb 92 pp 2-4

[Article by G.V. Konyushkov, A.I. Koblov, R.A. Musin, V.V. Utochkin, Saratov Polytechnic Institute and Perm Polytechnic Institute; UDC 621.791.76.01:537.226]

[Abstract] The shortcomings of the traditional methods of producing good permanent joints of functional ceramics, semiconductors, and glass ceramics in homogeneous and heterogeneous combinations by gluing, soldering, and diffusion welding in a vacuum are discussed and it is noted that pulsed pressure welding through electrically exploded conductors is free of these shortcomings while the joined parts, except for a thin surface layer, are not heated up. A lack of systematic data on this method prompted a thermodynamic analysis of the interaction of the explosion products of the 47ND alloy and tantalum with the SO-115M glass ceramics as well as a study of the welding method. The coat forming on the joined part surfaces serves as the welding layer; the coat formation mechanism is outlined and the energy and activity relations of the process are derived. The microhardness of the weld zone with a 5-6 μm welding layer is plotted. An experimental study carried out in a unit with a 2-10 kV controlled discharge and a 200 μF capacitor bank using quartz, glass ceramics, ruby, and silicon nitride samples welded through a Ni, Ta, Al, and 47ND alloy foil is described. The study established the principle patterns of pressure welding of nonmetallic materials through an electric explosion layer and made it possible to refine the procedures and equipment for making strong joints, both similar and dissimilar. Figures 4; references 8.

Radio-Frequency Fusion Welding

927D0241F Moscow SVAROCHNOYE PROIZVODSTVO in Russian No 5(691), May 92 pp 26-29

[Article by G.S. Tereshchenko; UDC 621.791.77.03]

[Abstract] The rising demand for welded products fabricated from stamped parts which cannot be made by conventional welding methods due to their low output and poor weld quality prompted the development of a new radio-frequency fusion welding technology which is especially

efficient for batch production of similar items. The method makes it possible to weld products from stamped parts along the flanged edge contour. The principal specification and basic principles of the method are summarized. For carbon steel most commonly used in such products, the current penetration depth varies from 5.75 to 0.43 mm at a frequency of 10-1,760 kHz. The design, specifications, and operating principle of the UVCh-1M, UVCh-25/0.44, UVCh-3, MVChK-2501, and UVChK8-25/0.44 RF fusion welding machines are presented. Vacuum tube oscillators which convert 50 Hz power main current to RF current with the help of rectifiers, three-electrode vacuum tubes, and tuned circuits are used as the power supply sources. The proposed method was exhibited at the Svarka-91 international fair held in Leningrad in 1991. Figures 5; tables 3; references 3.

Method of Engineering Static Strength Assessment of Welded Pipeline Girth Butt Joints

927D0241E Moscow SVAROCHNOYE PROIZVODSTVO in Russian No 5(691), May 92 pp 22-24

[Article by A.S. Zandberg, V.I. Khomenko, All-Union Scientific Research Institute of Pipeline Construction; UDC 621.791.052:539.4]

[Abstract] The shortcomings of GOST 6996-66 standards for testing pipe welded joints in the case of plastic collapse of the weld material prompted an analysis of the stability of plastic deformation of an individual pipe girth joint zone under the effect of residual plastic stresses affecting the onset of plastic flow. To this end, the plastic deformation instability under simple tension and loading diagrams in the complex stressed state of the welded joint material—an integral part of a larger structure—are analyzed and the dependence of the elasticity modulus of plastic hardening on the ratio of the yield strength:ultimate strength ratio is plotted for linear straining diagram approximation. The conditions of reaching the plastic state, a deformation increment corresponding to the tensile strength peak, and the maximum tensile stress in loaded pipe with a contact butt joint are examined and plotted. The results obtained for the welded joint metal are comparable to similar results produced for the base metal. The contact butt weld metal under a longitudinal tensile force is characterized by both a yield strength hardening and maximum load tolerance hardening determined from the plastic collapse condition. Consequently, the engineering static strength assessment method of girth welds must be based on the stability loss analysis of the plastic deformation process, i.e., plastic collapse. The geometrical design characteristics and residual stress features of flash resistance welded pipe joints make it possible to attain the necessary structural strength and transfer the failure zone to the base metal. Figures 4; references 6: 5 Russian, 1 Western.

Girth Welded Joint Strength of Tubes for Sour Gas From Molybdenum Steel

927D0241D Moscow SVAROCHNOYE PROIZVODSTVO in Russian No 5(691), May 92 pp 17-18

[Article by I.A. Romanova, A.G. Mazel, Ye.V. Lopatin, N.I. Klimova, All-Union Scientific Research Institute of Pipeline Construction; UDC 621.791.052:539.4]

[Abstract] The metal hardness of girth welded joints in sour gas pipes from molybdenum steel manufactured by the Nippon Kokan Company (NKK) for the Astrakhan Gas Processing Plant is investigated experimentally using 168.3 x 9.5 mm tube samples welded by several different methods: Fox Cel downhill and OZS/VNIIST-26. An HV_{10} 275 hardness is noted in the heat affected area (ZTV) which exceeds the maximum permissible level of 248 HV. This fact prompted a study of effect of the linear welding energy, preheating, and interlayer temperature on the weld root hardness and an examination of the heat affected area hardness near the bead which is not affected by the heat of the subsequent layers and where hardness reaches peak levels. The cumulative effect of heating and interlayer temperature under cellulose electrode welding on the weld root hardness during the bevel filling and the effect of the electrode coating type on the weld root hardness are plotted. An analysis shows that preheating decreases the heat affected area's hardness in the first weld layer by 10-12% thus lowering the probability of cracking under the bead, especially when using cellulose-coated electrode while the root weld hardness decreases by 30-40% due to the annealing effect of the subsequent layers. The importance of maintaining a high interlayer temperature during welding for further decreasing the heat affected area bead hardness by 15% without affecting the metal hardness in the weld root is stressed. Figures 5; tables 2; references 4.

Welding Characteristics of Polyethylene Tubes Under Extreme Temperature Conditions

927D0241C Moscow SVAROCHNOYE PROIZVODSTVO in Russian No 5(691), May 92 pp 11-14

[Article by B.F. Vindt, I.V. Sbarskiy, All-Union Scientific Research Institute of Pipeline Construction; UDC 621.791.46:678.5./8]

[Abstract] The need for heated-tool butt-welding of polyethylene tubes under extreme temperature conditions (from -40 to +50°C) in building various oil and gas installations in diverse regions and the constraints imposed on such operations as well as a lack of relevant instruction manuals prompted an investigation into the peculiar features of polyethylene tube welding under such conditions. It is shown that the principal condition for attaining strong butt welds in thermoplastic tubes is to allow the rheological processes to run their course during the upsetting and that the development of an equivalent thermal condition at the upsetting moment during welding at extreme temperatures makes it possible to make welded joints whose quality is equal to, or exceeds, that of tubes welded at a normal temperature but with the same thermal conditions. The dependence of the heated tool temperature and the coefficient β which depends on the wall thickness and tube diameter on the ambient temperature, the radial wall hardness variation in the low-pressure polyethylene (PND) tube, and the axial welded joint hardness variation at various temperatures are plotted. The results of tensile strength, bending strength, and cracking resistance tests of various low-pressure polyethylene tubes at different temperatures are summarized. The tests reveal that there is no difference in the loss of structural strength of sections welded at +20 and -20°C whereby the stress in the tensile butt cross section reached 23 MPa, i.e., close to the LPPE yield stress. The findings confirm that the development of equivalent

thermal conditions in the tube ends at the upsetting moment ensures an adequate welded joint properties within a -40 to +50°C range. Figures 3; tables 1; references 14: 11 Russian, 3 Western.

Wear Resistant Surfacing Materials and Composites for Hardening Friction Surfaces Under Abrasive and Hydroabrasive Wear Conditions

927D0241B Moscow SVAROCHNOYE PROIZVODSTVO in Russian No 5(691), May 92 pp 7-9

[Article by N.A. Grinberg, A.B. Arabey; UDC 621.791.92.04:621.922.025.004.6]

[Abstract] The factors which determine the resistance of surfacing alloys to abrasive and hydroabrasive wear and the basic premises used in developing high-alloy surfacing and composite materials are discussed. The correlation between alloying, fine structure, and alloy resistance to abrasive and hydroabrasive wear is investigated and various carbon-bearing chromium and boride alloys with dopants developed for mechanized and manual arc deposition are examined. The alloys are tested for abrasive impact resistance to soil in a Rotor machine; at the same time, 16 samples surfaced with various materials are tested. The chemical composition of the experimental alloys and the test results are summarized. Samples surfaced by YuK-12 and YuK-14 electrodes show that their abrasive wear resistance exceeds that of sormite by 1.8 and 4.8 times, respectively. The conclusion is drawn that in order to extend the service life of parts operating under abrasive impact wear, materials with carboboride (SP-U10Kh7GR1 sintered tape) and carbonitride (PP-Np-100Kh4G2AR powder wire and VSN/OZN-7 and VSN/OZN-9 electrodes) are preferable; for hydroabrasive wear, the VSN-14 and VSN/OZN-9 electrodes are suitable. The study confirmed the possibility of producing surfacing composites by arc deposition and the efficiency of using a mixture of TiB_2 and CrB_2 particles as the hardening phase. Figures 2; tables 2.

Welding of Mo-Alloyed Tubes for "Sour" Gas and Crude

927D0241A Moscow SVAROCHNOYE PROIZVODSTVO in Russian No 5(691), May 92 pp 3-4

[Article by A.G. Mazel, N.G. Goncharov, A.Yu. Sinayskiy, All-Union Scientific Research Institute of Pipeline Construction; UDC 621.791.753:621.643]

[Abstract] The shortcomings of the low-carbon corrosion-resistant tubes with a limited sulfur and manganese content usually used abroad for sour gas pipelines (ladle refined by argon blasting) is discussed and it is noted that the main criterion used for estimating the tube welded joint suitability for sour gas and crude is the low weld and near-weld metal hardness; according to NACE standards, it should not exceed 22 HRC (248 HV). This requirement cannot be easily met for Mo-containing tubes; this factor prompted lab and test bench studies of three tube samples with 0.24, 0.25, and 0.26% Mo concentration; the concentration of the remaining alloying additions and the mechanical properties of the tubes are summarized. The weld structure is examined in samples welded by two methods: a butt weld made solely by cellulose-coated electrodes by downhill welding; and a weld root layer and hot pass made by cellulose-coated electrodes by downhill welding while the subsequent weld layers are made by basic-coated electrodes and uphill welding. The welding versions, heat treatment conditions, and maximum HV hardness before and after heat treatment (high tempering) are summarized and the hardness distribution in the working part of the sample is plotted. Subsequent corrosion tests are carried out for 720 h to examine the hard structure forming in the heat affected area (ZTV) and measure the hardness distribution. The samples display low tendency of the hard structure developing in the weld area to corrosion cracking in an H_2S medium. Full-scale tests are conducted in Russia and Japan for 720 h in a medium with 25% H_2S and 15% CO_2; the results also reveal no corrosion damage to the welded joints. Thus, the development of hard segments in the heat affected area with an up to 270 HV hardness may be allowed without any loss of corrosion resistance of welded joints of Mo-alloyed steel. Figures 2; tables 2; references 4.

Stability of Acoustic Emission Parameters With Different Thicknesses of the Transducer-Object Contact Layer

927D0160A Kiev TEKHNICHESKAYA DIAGNOSTIKA I NERAZRUSHAYUSHCHIY KONTROL in Russian No 1, 92, Jan-Feb-Mar 92 pp 27-31

[Article by V. I. Ivanov and V. A. Mirgazov, Scientific and Production Association of the Central Scientific Research Institute of Machinery Manufacturing Technology, Moscow, and Scientific and Production Association of Cryogenic Machine Building; UDC 621.791.052.08: 620.179.16]

[Abstract] Each element of the acoustic data channel, which consists of the test object, the contact layer, and the acoustic emission transducer, is a source of certain distortions which affect parameters of the acoustic emission signal. It was of practical interest to know how acoustic emission parameters change depending on variations in the thickness of the contact layer, within limits which are common for acoustic testing. A calculation experiment was designed which took into account the input signal for the AE transducer which describes a single activating event of the AE source, the input signal's spectrum, the signal's spectrum on output from the AE transducer, and the reaction of the transducer. The experiment was conducted with a Dunegan Endevco S750B resonance-type piezoelectric transducer containing a piezoelectric plate, a liner, and a protector, which together with the test object and the contact layer constituted a five-layer vibrational system loaded to a semi-infinite space through an idealized contact layer with parallel boundaries. To evaluate how stable AE parameters remain when the contact layer's thickness changes, a formula was used which described the mechanical coefficient of conversion of sound pressure for the five-layer system. Transmission characteristics (amplitude and phase) of the test object-transducer system were determined at 10 different fixed thicknesses of the contact layer ranging from 0 to 10 mm. Next, the thickness of the contact layer was varied and the corresponding pulse characteristics were determined. It was found that for thicknesses up to 1 mm, pulse characteristics vary little; when the thickness is increased to 10 mm, significant differences appear. From the shape of curves of AE parameters plotted against contact layer thicknesses, it is

possible to discern three intervals: 0-0.1 mm, 0.1-1 mm, and 1-10 mm, among which the first is noteworthy. In it the AE parameters have the smallest spread of values, which corresponds to a test object surface with roughness in the range 0.2-100 micrometers. Calculations showed that the contact layer thickness has a definite effect on recorded parameters of AE signals, and the greatest effect is produced by a thickness in the range 0.1-1.0 mm. Here the change in pulse amplitude reaches 17%, and the change in the number of spikes reaches 30%. Considering that in real conditions parameters of AE signals vary within significantly broader limits, the effect of the contact layer thickness cannot be considered substantial, which is connected with the fact that operating frequencies in the AE method are relatively low, and there is no need to place special requirements on the surface finish.

Peculiarities of Redistribution of Residual Stresses in Welds Under Cyclic Compression

927D0160C Kiev TEKHNICHESKAYA DIAGNOSTIKA I NERAZRUSHAYUSHCHIY KONTROL in Russian No 1, 1992, Jan-Feb-Mar 92 pp 38-43

[Article by Ye. K. Dobykina, A. G. Burenko, O. I. Gushcha, P. P. Mikheyev, and V. K. Kot, Institute of Electric Welding im. Ye. O. Paton, Ukrainian Academy of Sciences, Kiev; UDC 621.791.052:539.43]

[Abstract] Experiments were done to study the redistribution of residual weld stresses under the action of primarily compressive external alternating loading. Residual stresses were investigated in welds made in models which reproduced welded assemblies of jibs on two different models of powerful draglines. The models contained four types of welds: butt attachment of a trapezoidal shape; attachment of a lengthwise rib with a fillet weld along the contour; attachment of a plate with a fillet weld along the contour; and attachment of a cross rib with end lap fillet welds. Residual weld stresses were measured by the nondestructive acoustic method. Parallel measurements of initial residual stresses were made in an identical model using the destructive method with strain transducers. Measurements were made in places where fatigue cracks originated and propagated in the course of fatigue tests. Initial residual weld stresses and also stresses established after different levels of external compressive loading were measured. The first level of loading corresponded to stresses at which fatigue cracks originated and propagated during tests under compression starting at zero. It was found that after compressive loading and relaxation, in most cases there occur changes in the levels of both compressive and tensile residual weld stresses, and the degree and character of these changes differ significantly for different welds. Change in the initial level of residual weld stresses takes place during the first loading cycles. Change in the initial level of tensile residual stresses under external compressive loading takes place mainly due to the change in initial compressive residual stresses, which compensate the tensile stresses. Initial compressive residual stresses change substantially only when the sum of stresses from external compressive loading and residual compressive stresses exceeds the material's yield point under compression. In all types of welds after compressive loading up to 160 MPa, tensile residual stresses in zones of concentrators are not totally removed, and in some types of welds these stresses remain at practically the initial level. In butt welded trapezoidal shapes, tensile residual stresses in zones of concentrators do not decrease even after high compressive loading. This is because initial compressive residual stresses have comparatively low levels, and zones of their distribution are rather distant from zones of concentration of operational stresses. It is characteristic that welds of the butt-welded shape type developed fatigue cracks in all cases in tests under compression with stress levels of 120 to 240 MPa, and they demonstrated significantly shorter service life and lower durability limits than the other types of welds studied. The experiments confirmed the thesis that for many types of welds under compressive loading in a range of nominal stresses typical of the multicyclic field, tensile residual stresses virtually do not change.

Acoustic Emission Diagnostics and Testing of the Quality of Welds in Vessel-Type Structures

927D0160F Kiev TEKHNICHESKAYA DIAGNOSTIKA I NERAZRUSHAYUSHCHIY KONTROL in Russian No 1, Jan-Feb-Mar 92 pp 60-64

[Article by V. K. Shukhostanov, Severodvinsk; UDC 621.791.052:539.4]

[Abstract] Early acoustic emission diagnostics of welds—meaning directly in the welding process and in the period just after welding—is advocated as a way to make production more efficient and to improve the quality and reliability of vessel-type structures. It is explained that with more and more nondestructive tests being performed after welded structures are completed, the volume of corrective repairs of welds is increasing likewise. With existing technology, the approach is to test completed structures and fix welding defects after the weld and defects have been formed. Early stages of defect formation—the very physical processes involved in origin, growth and development of welding defects—usually are not covered by testing procedures. It is explained that in multiple-pass welding, which is used widely for vessel-type structures, each newly made bead experiences a compression-stretching cycle, and nearby beads are subject to cyclic loading. In the process, the weld endures layer-by-layer (bead-by-bead) local cyclic loading with the cycle's amplitude being equal to the yield point of the metal, and ultimately the weld is loaded with residual welding stresses which also reach the yield point. During welding there is a normal, background acoustic emission whose sources are processes of fusion, crystallization, phase and structural transitions, plastic deformation, and formation of surface oxide films. This acoustic emission's parameters and regularities should be the same over the whole length of the weld. Processes of the origin, formation and development of welding defects give rise to an extra acoustic emission on top of the normal, background emission. Recording of this extra acoustic emission at the earliest stages of defect formation makes it possible to reveal welding defects in real time and to monitor processes of defect formation and control the welding process. Early acoustic emission diagnostics can be based on four principles: detection of defects as they originate; localization of defects; acting on defect formation processes at the stage of origin (immediate correction); and diagnostics in the process of formation and stabilization of residual stress fields. All four principles of early acoustic emission diagnostics can be implemented directly in the welding process simultaneously.

Predicting the Limiting State of Pressure Vessels According to Acoustic Emission Signals

927D0160G Kiev TEKHNICHESKAYA DIAGNOSTIKA I NERAZRUSHAYUSHCHIY KONTROL in Russian No 1, Jan-Feb-Mar 92 pp 64-71

[Article by V. A. Strelchenko, S. N. Pichkov, and V. V. Danilin, Institute of Problems of Strength, Ukrainian SSR Academy of Sciences, Kiev, and Experimental Design Bureau for Machine Building, Nizhniy Novgorod; UDC 629.179:512.21]

[Abstract] Wider use of acoustic emission testing of structures under loads is being held back by the lack of a one-to-one correspondence between mechanical characteristics of materials which are responsible for failure and parameters of AE signals. Studies were conducted with the following set of goals: to determine the AE parameter which is the most informative relative to deformation and failure of selected materials; to construct a linear regression model of the interrelationship between the kinetics of mechanical stresses and the kinetics of the AE parameter which is found to be the most informative; to investigate AE signal parameters from positions of random process theory to create an algorithm for predicting AE parameters; by predicting AE parameters and using the established one-to-one correspondence, to determine the limiting values of mechanical characteristics of materials given the presence of information about AE parameters which correspond to the initial sector of deformation; and to adapt the methods developed to predict the limiting state of pressure vessels according to AE signals. An AE parameter was selected which had a high degree of linear relation with the mechanical characteristic of the test material and a high degree of statistical stability as compared with other AE parameters. This operative parameter turned out to be a parameter of the energy type, whose value can be interpreted as the electrical equivalent of the energy dissipated by the test specimen by the x-th moment in time from the moment loading of the specimen begins. The problem of constructing a regression model of the AE parameter vs. mechanical stress was solved using a modified least-squares method. The solution makes it possible to regenerate the kinetics of mechanical stresses along the trajectory of the AE parameter. Actually, the solution of the problem and determination of coefficients of the regression model are presupposed, and from the known trajectory of the AE parameter it is necessary to determine unknown values for mechanical stress. Assuming that it is possible to predict the AE parameter according to its starting sector corresponding to the initial stage of loading of the test specimen, it is possible to determine the values of mechanical stresses which correspond to the limiting state of the specimen. A linear-iterative prediction method was used which makes it possible to find unknown values for a yet unknown trajectory of the AE parameter in the form of linear combinations of values of previously known trajectories. Results of evaluating the breaking mechanical stresses for three different materials are presented. The method makes it possible to predict the limiting state of materials according to AE signals recorded at an early stage of deformation of materials, and it can be used for technical diagnostics and predicting the limiting state of shell-type structures.

Areas of Use of the Acoustic Emission Effect in Making Welded Structures

927D0160H Kiev TEKHNICHESKAYA DIAGNOSTIKA I NERAZRUSHAYUSHCHIY KONTROL in Russian No 1, Jan-Feb-Mar 92 pp 77-80

[Article by V. I. Panov and I. Yu. Iyevlev, Ural Heavy Machine Building Production Association, Yekaterinburg, Central Scientific Research Institute of Machine Building, Yekaterinburg; UDC 621.791.052:620.179.16]

[Abstract] Information on the ability of acoustic emission testing to detect crack formation in the manufacturing stage of large welded structures for heavy machinery is presented in the form of a long table. The information is the result of many years of use by the Ural Heavy Machine Building Production Association of equipment developed by the Central Scientific Research Institute of Machine Building. The equipment helped to define the possibilities of the AE method in testing large thick-walled structures over the course of the whole manufacturing cycle. The AE effect is used in laboratory tests and as a method of testing during technological operations on real structures. It helps to determine the onset of the stage of pre-failure and growth of cracks, and to diagnose the durability of thick-walled welded structures of heavy machinery at the completion of their manufacture. The table lists key failure factors (deformation of the metal of blanks or welds, change of position of pieces being welded, stresses, thermodynamic aging, etc.), technological operations associated with them, and whether the AE method is effective or not effective in detecting crack formation during these operations.

Telemetry System for Evaluating Stressed State of Welded Structures in Hard-to-Reach Places

927D0160I Kiev TEKHNICHESKAYA DIAGNOSTIKA I NERAZRUSHAYUSHCHIY KONTROL in Russian No 1, Jan-Feb-Mar 92 pp 81-84

[Article by S. K. Fomichev, V. G. Tatarnikov, V. A. Stechenko, A. A. Chernata, I. M. Zhdanov, V. V. Batyuk, V. A. Veligin, and A. V. Pulyayev, Kiev Polytechnical Institute; UDC 539.319]

[Abstract] The Kiev Polytechnical Institute developed a telemetry system for periodic testing of the most highly stressed parts of welded structures in hard-to-reach places such as pipelines in swampy areas. The multichannel remote measurement system consists of a base unit worked by an operator and the necessary number of outlying measurement units installed at testing sites. The base unit contains an address generator, a transceiver and a pulse counter. Each measurement unit contains a transformer-type superposed quadrupole magnetoelastic mechanical stress transducer, a voltage-to-frequency converter, a transceiver, an address decoder, and an operational control circuit. The system's measurement error does not exceed +/-15% in 82% of measurements. From the base unit the operator gives the required receiver address, which goes to the transmitter in code form and an amplitude-manipulated signal is sent at about 27 MHz. All outlying measurement units are initially in standby mode with low power consumption from batteries. The address decoder has power continuously on, and when addresses match, the control device turns on power to the transducer,

the voltage-to-frequency converter, and the transmitter. The measured physical value is converted to the frequency of pulses which are sent out into the airwaves for a period of 5 seconds. The amplitude-manipulated signal goes from the antenna to the receiver of the base unit and on to the pulse counter. The outlying measurement unit contains a decoder, a transducer power-supply board, and a receiver and transmitter placed in an airtight metal case measuring 320x140x40 mm. Power supply components are located in another case. Cassettes with power components are replaced when power runs low (approximately once a month). The base unit is contained in a case 400x250x80 mm. Power is from a 220 V grid. Proving trials have demonstrated good reliability of the system at distances of measurement units from the base unit of up to one kilometer.

Higher Utilization Efficiency of Sodium Sulfide and Its Substitutes in Flotation of Sulfide Ores

927D0190N Moscow TSVETNYYE METALLY in Russian No 5, May 92 pp 69-71

[Article by L. A. Glazunov, State Research Institute of Nonferrous Metals; UDC 622.765]

[Abstract] Nonferrous metallurgy's demand for sodium sulfide for flotation of ores is not being met by domestic suppliers, and hard currency is not available to import it. Waste products of a number of industries can be used as substitutes for sodium sulfide. Among them are sodium hydrosulfide and sulfurous-alkaline wastes of oil refineries. The latter have been found by laboratory and industrial studies to be a suitable substitute for sodium sulfide, and even somewhat better in extracting copper and molybdenum. Because they are not environmentally safe, it is recommended that vacuum flotation machines with limited air feed be used with these substitutes, and that these machines be enclosed to prevent escape of gaseous reaction products. Other considerations include the measuring of reagents by optimum values of redox and electrochemical potentials.

Effect of Particular Factors on Fuel Consumption in Sinter Production

927D0218A Dnepropetrovsk METALLURGICHESKAYA I GORNORUDNAYA PROMYSHLENNOST: NAUCHNO-TEKHNICHESKIY I PROIZVODSTVENNYY SBORNIK in Russian No 2, Apr-Jun 92 pp 1-3

[Article by A. Z. Krizhevskiy, Donetsk Scientific Research Institute of Ferrous Metallurgy; UDC 622.788.36:[662.613.13:699.014.84]:008.5]

[Abstract] The industry standard being used to determine solid fuel consumption norms at sintering plants in Ukraine takes account of the effect of the sinter mixture's composition and of the process parameters on the change in fuel consumption when there are variances from baseline values in consumption of blast furnace dust, limestone, lime, and iron monoxide scale in the sinter, as well as in the depth of the burden layer and its temperature. However, this standard is said to be lacking in that it does not take into account the effects on fuel consumption of changes in consumption of the overall mass of the sinter mixture (without the fuel) and of sinter return and iron-containing slurry. Numerical values were calculated for coefficients that take into account the change in consumption of sinter mixture, sinter return and iron-containing slurry to supplement the existing industry standard for determining norms of fuel consumption in sintering of iron-ore concentrates. Also calculated is the change in fuel consumption for each 0.1% weight increase of iron in the sinter.

Briquetting Manganese Concentrates by Hot Pressing

927D0218B Dnepropetrovsk METALLURGICHESKAYA I GORNORUDNAYA PROMYSHLENNOST: NAUCHNO-TEKHNICHESKIY I PROIZVODSTVENNYY SBORNIK in Russian No 2, Apr-Jun 92 pp 3-4

[Article by V. F. Moroz and V. S. Baraban, Institute of Ferrous Metallurgy; UDC 622.788.32:622.341.2]

[Abstract] Briquetting of manganese concentrates by means of hot pressing was seen as a way to overcome drawbacks of the traditional sintering method, namely, reduced furnace efficiency and high dust formation. The briquetting process was tested on a laboratory installation which allows finely dispersed materials to be press-formed in a graphite mold at temperatures up to 1000 degrees C. The briquets produced have a cylinder shape 14 mm in diameter. Tests showed that it is possible to produce briquets at a temperature of 700-800 degrees C and pressing pressure of 100 MPa. The strength properties of these briquets meet the requirements of ferroalloy production. Their density is approximately 2.1 g per cubic cm, and their compression strength is 3.4-4.5 kN per briquet. In the process, moisture from hydrates is removed and there is dissociation of manganese carbonates, which improves the properties of briquets and should give them higher melting efficiency in furnaces.

Investigation of Composition and Structure of Briquets Made From Mill Scale

927D0218C Dnepropetrovsk METALLURGICHESKAYA I GORNORUDNAYA PROMYSHLENNOST: NAUCHNO-TEKHNICHESKIY I PROIZVODSTVENNYY SBORNIK in Russian No 2, Apr-Jun 92 pp 10-13

[Article by Z. I. Nekrasov, V. F. Moroz, V. I. Negoda, B. G. Rudovskiy, Institute of Ferrous Metallurgy; UDC 620.191.32:622'188]:[669.017.3:620.18]

[Abstract] Results of investigation of reduction treatment and briquetting of mill scale and study of the phase composition and structure of prepared sinter mixture and briquets are presented. Reduction of the scale was done in a laboratory rotary furnace at 800-1000 degrees C, with natural gas and gas coal used as reducing agents. Briquets made of scale with different levels of reduction were produced on a laboratory hot-pressing installation at 850 degrees C and pressure of 108 MPa. Phase composition and structure were examined optically with a microscope and with a scanning electron microscope, and etching with hydrochloric acid solution in alcohol was used to determine structure. It was determined that treatment of mill scale to make strong briquets consists in reducing ferric oxides to wustite or metallic iron, and that coal with a high content of volatile matter or natural gas can be used as the reducing agent. Briquets with a strength of 10 kN and higher can be produced at a temperature of 850 degrees C and pressure of 108 MPa from a sinter mixture reduced with coal at 850-1000 degrees, or with natural gas at 800-1000 degrees C. Wustite-bound briquets which are partially metallized (up to 30%) can be used in blast furnace production, and with higher levels of metallization they can be used for steelmaking. Because mill scale is a comparatively pure material, it is economically advantageous to use it in the form of metallized briquets for steelmaking.

More Effective Crushing of Flooded Rock in Open-Pit Mines by Draining Blast Holes With the Aid of Bottom Charges

927D0218F Dnepropetrovsk METALLURGICHESKAYA I GORNORUDNAYA PROMYSHLENNOST: NAUCHNO-TEKHNICHESKIY I PROIZVODSTVENNYY SBORNIK in Russian No 2, Apr-Jun 92 pp 39-40

[Article by P. I. Fedorenko and A. P. Pashkov, Krivoy Rog Mining Institute, and A. F. Gribovoda, Dokuchayevsk Flux

and Dolomite Combine; UDC 622.271.35.004.12: 622.235.213.2]: 622.58.016.25]

[Abstract] Results of studies are presented in which blast holes were drained by setting bottom charges in open-pit mines. The effect of this was examined for the dilatancy softening of rock mass in the zone around a stope and for water flow in blast holes. On the basis of industrial tests, a method was developed for draining blast holes which prevents damage to the mouths of blast holes and which creates conditions for good plugging of blast hole walls so that non-waterproof (or partially waterproof) explosives can be used. The method makes possible more uniform crushing of rock and reduces the number of large pieces of rock (more than 400 mm) by half.

Testing of a Metal Shaft Lining as a Local Ground in Underground Workings of Manganese Mines of the Nikopol Deposit

927D0218G Dnepropetrovsk METALLURGICHESKAYA I GORNORUDNAYA PROMYSHLENNOST: NAUCHNO-TEKHNICHESKIY I PROIZVODSTVENNYY SBORNIK in Russian No 2, Apr-Jun 92 pp 67-69

[Article by M. V. Gorbachev, Ukrainian Mining Industry Concern, G. S. Linetskiy, Marganets Mining and Ore Enrichment Combine, A. F. Martynov, Dnepr District of Ukrainian State Mine Inspection Agency, and A. Z. Nikolaychuk, Dnepropetrovsk Mining Institute; UDC 621.316.991:622.281.5]:65.012.8]

[Abstract] Results of testing of a metal shaft support lining as a natural ground for local grounding of mineshaft electrical installations are presented. Tests were conducted in mines of the Marganets Mining and Ore Enrichment Combine. Use of the metal shaft lining to provide for local grounding of electrical installations was shown to be feasible and effective. It substantially reduces labor costs in setting up protective grounding, eliminating the need to drill holes in shaft walls for grounding rods and to prepare special mixtures for setting rods. Grounding elements of the lining are easily moved and installed at new sites of underground workings.

Platinoids and Gold in Diagenetic Pyrite Concretions of Jurassic Shale on South Slope of Central Caucasus

927D0229A Moscow RAZVEDKA I OKHRANA NEDR in Russian No 2, Feb 92 pp 2-3

[Article by A.G. Zhabin, N.S. Samsonova, Yu.G. Kosavets, Institute of Rare Element Mineralogy, Geochemistry, and Crystal Chemistry; UDC [546.9+546.59]: [553.061.16: 549.324.31: 552.124.4] (470.6)]

[Abstract] Nontraditional and virtually new geological formations where platinum group metals are being concentrated primarily in sedimentary and metamorphized sedimentary rock rich in organic matter are reported to the Fifth International Platinum Symposium held in Finland in 1989 and it is speculated that the enclosing rock in the Jurassic shale on the south slope of the Caucasus could contain an accumulation of platinoids. Attempts to prove this premise starting with the levels rich in diagenetic pyrite concretions are described. A lithogeochemical study is conducted in the Tskhenis-tskali and Zeskho river basins and pyrites are studied by Yu.G. Kosavets in an experimental laser unit for local emission spectral analysis using point pulse probing of individual mineral grains or their profile measurements in polished samples. The spectra are recorded by an STE-1 diffraction spectrograph within a 200-700 nm band. A typical pyrite fine-grain elliptical concretion in cleavaged black shale is shown and the concentration of Pt, Pd, Au, and other elements in these pyrite concretions is summarized. It is noted that the poor analytical base and the lack of secure methods are the greatest obstacle to examining new potential natural platinoid sources. The pyrite's ability to accumulate and absorb precious metals at any period in its formation and subsequent existence and its mechanisms are outlined and the role of transverse Caucasian fractures in the ore concentration on the concretion pyrite barrier is noted. The geological factors which determine the form of potential ore zones, mostly the form of primary geochemical anomalies, are formulated. Figures 1; tables 1; references 7: 5 Russian, 2 Western.

Gold Ore Deposit Exploration by Secondary Ammonium Scattering Aureoles

927D0229B Moscow RAZVEDKA I OKHRANA NEDR in Russian No 2, Feb 92 pp 8-10

[Article by S.A. Milyayev, V.B. Chekvaidze, A.A. Demeshko, L.V. Lapchinskaya, Central Scientific Research Institute of Rare and Precious Metal Geological Surveying and Kharkov State University; UDC 550.84.092.2:553.411]

[Abstract] The use of new elements and their compounds which possess high indication properties, such as the ions of ammonium accumulating in the ore deposit neighborhood is discussed and it is noted that in central Nevada, the NH_4^+ ion concentration exceeds 3% in some of the deposits. The reasons for the elevated ammonium ion concentration in gold ore deposits and the methods of measuring it, particularly the potentiometric method which is characterized by high speed, as well as the domestic and foreign potentiometers used for this purpose are examined. The gold content and ammonium concentration in secondary scattering aureoles of Au-Ag deposits, the linear yield ratios of ammonium and gold ions in secondary scattering aureoles, and potentiometric curves across the profile of a Au-Ag deposit are plotted. The high exploration and surveying potential of the salt scattering aureoles of the components which accompany gold and silver deposits and the advantages of analyses employing ion-selective electrodes, especially their low cost, high speed, and the possibility to produce results directly in the field, make it possible to use the method in exploration and evaluation procedures within ore deposits with known types of gold mineralization as well as in assessing geochemical anomalies. Figures 3; references 5: 4 Russian, 1 Western.

Characteristics of Leakage Flux Formation in Cryolite Zone Landscapes in Northeast Russia

927D0229C Moscow RAZVEDKA I OKHRANA NEDR in Russian No 2, Feb 92 pp 10-12

[Article by V.A. Kononov, SVKNII at the Far Eastern Department of Russia's Academy of Sciences; UDC 550.84.092:553.3(571.651)]

[Abstract] The quantitative characteristics of the leakage fluxes which point toward the peculiar features of their formation under varying landscape and geochemical conditions in the cryolite zone are investigated. To this end, the leakage flux of Au, As, Ag, Pb, Cu, Zn, Mo, and Sn manifestations of the Oloyskaya zone, South Anyuyskiy downwarp, and Anyuyskiy folding zone are measured. The study of the flux formation characteristics of the ore complex elements is based on analyzing the variations in the α' and β' alluvium slope coefficients as a function of the landscape and geochemical conditions and dynamic phases of the water course development. The measurement procedure and the geochemical processes occurring within various terrain formations are outlined and three dynamic phases of water course development—instrative, perstrative, and constrative—are identified and summarized for Au, As, Ag, Pb, Cu, Zn, Mo, and Sn. An analysis of the characteristics of leakage flux formation make it possible to derive formulae for the slope coefficient and leakage flux yield. The outcome of the study makes it possible to establish a correlation between the dynamic phases of the water course development, terrain types, and geochemical landscapes on the water course valley slopes and reveals a consistent increase in the amount of material on the nearest slopes in the alluvium sample in the direction from the instrative to constrative phase through the perstrative phase. Moreover, an increase in the role of the nearest slope material approximates the element content in the alluvium to its concentration in the alluvium-deluvium of the nearest slopes, making it possible to calculate the leakage flux yield. The findings complement known data on the leakage flux formation and enable the scientists more efficiently to interpret the results of geochemical surveying. Tables 1; references 10.

Digital Processing and Interpretation of Navigation Charts in Littoral Placer Forecasting

927D0229D Moscow RAZVEDKA I OKHRANA NEDR in Russian No 2, Feb 92 pp 17-19

[Article by A.M. Belinskiy, N.I. Korchuganova, Moscow Geological Surveying Institute; UDC [527(084.3): 681.3.01]: 553.068.56.001.3.01]

[Abstract] The origin and characteristics of littoral alluvial deposits and the difficulties of predicting them as well as the need to take into account the role of various factors of the placer formation at different forecast stages are discussed. It is noted that regional geophysical data, aerial and space photographs, and navigation charts are the principal sources for identifying the structural plan of deposits and the results of digital processing of navigation charts of the northern segment of the Penzhinskiy Bay of the Sea of Okhotsk performed by the authors using a Pericolor-200 E display system are reported and a model of its structural and geomorphological makeup is proposed. The original image is smoothed using low-frequency filtering with a 3x3 pixel window in order to decrease random errors. The findings are used as the basis for a structural geomorphological chart showing the main sea bottom elements, the coastline, large rivers, etc. This interpretation of the navigational charts and available geological and geophysical materials makes it possible to develop a sound model of the structural plan of the bay segment and to outline the structural and geomorphological traps of the likely placer formation. Such proximate analyses are especially efficient at the early design stage. Figures 1.

Precious Metals in Refining Products of Various Types of Mercury Ore Deposits

927D0229E Moscow RAZVEDKA I OKHRANA NEDR in Russian No 2, Feb 92 pp 19-22

[Article by A.A. Bogdasarov, V.A. Stepanov, R.O. Berzon, Brest State Teachers College imeni A.S. Pushkin and Central Scientific Research Institute of Geological Surveying; UDC 553.499:669.213'223]

[Abstract] All principal commercial mercury deposits are divided into three genetic classes—plutogenic, telethermal, and volcanogenic—and it is noted that gold and silver or at least their elevated concentrations are observed in virtually all types of mercury deposits but only the telethermal ones contain commercial quantities of precious metals. The ores from the main commercial types of mercury deposits are investigated in order to examine the gold content of mercury ores and the associated silver concentration as well as the precious metal distribution in the enrichment and roasting products; in so doing, special attention is focused on the gold incidence forms and the locations of its concentration. The mineral types of the principal auriferous mercury deposits and their geological and technological characteristics are summarized and the deposit mineralization is reviewed. The precious metal concentration in the mercury ore refining products is analyzed and the mercury mineralization localization and the occurrence of gold are examined. It is noted that although available experience with ore processing by the chemical and hydrometallurgy technology makes it possible to recover Hg, Au, and Ag simultaneously, it has not found applications in domestic practices. Figures 1; tables 1; references 7: 6 Russian, 1 Western.

Gold in Jasperoid-Type Sb-Hg Ores and Enclosing Rock Deposits

927D0229F Moscow RAZVEDKA I OKHRANA NEDR in Russian No 2, Feb 92 pp 22-24

[Article by V.V. Rogalskiy, South Kyrgyz Mining Expedition; UDC [546.59:553.497.2'499]:550.42(575.13)]

[Abstract] The prominent role of hydrothermal-metasomatic Hg-bearing deposits with finely disperse Au in the gold industry since the discovery of the Carlin deposit in the United States is noted and the morphostructural types of gold mineralization within the Sb-Hg ore fields of the south Fergana belt are classified; in some deposits, the gold concentration reaches 1-5 g/t yet attempts to assess it have thus far been unsuccessful. The origin and structure of the south Fergana Sb-Hg belt are discussed and the formation appurtenance and gold concentration characteristics of the Sb and Hg deposits in the south Fergana area are summarized. The gold concentration in Sb-Hg ores and enclosing rock in Jasperoid-type deposits in south Fergana and the ore manifestation patterns are analyzed and the deposit and manifestation distribution are examined. The findings point toward a good outlook for identifying a number of gold mineralization types in ore fields in the south Fergana area and

confirm a well developed gold mineralization. It is stressed that since current ore and concentrate refining processes call for shipping the auriferous cake for subsequent recovery at the gold mining works, accurate accounting of the gold and associated component concentration make it possible to raise the deposit's value. Tables 1.

Au:Ag Ratio Versions in Chadak Ore Field Deposits

927D0229G Moscow RAZVEDKA I OKHRANA NEDR in Russian No 2, Feb 92 pp 24-27

[Article by T.M. Mazhidov, Uzbek Gold Production Association; UDC [546.59+546.57].009:553.04]

[Abstract] The increasing urgency of assessing the flanks and deep levels of the Chadak deposit prompted an attempt to use the value of the Au:Ag ratio for estimating the mineralization depth outlook and clarifying the still undecided formation type of the Chadak deposit as an objective basis for comparing them to similar entities of volcanic and plutonic belts. The Au:Ag ratio has been extensively used for over 50 years both at home and abroad for classifying Au-Ag deposits and metallogenic formations. The reasons for using the Au:Ag ratio are explained and the geological characteristics of the Chadak ore field and its formation features are discussed in detail and ore-bearing zones and ore veins in the Chadak ore field as well as the Au:Ag ratio variations in commercial veins of the Chadak deposits as a function of their depth are plotted. The Au:Ag values in commercial veins, lots, and deposits in the eastern and western flanks of the ore field are summarized and the commercial veins are divided into three principal categories according to the Au:Ag ratio. The conclusion is drawn that the principal factors affecting the Au:Ag ratio are the correlation of productive associations and the depth of the vein erosion shearing while the ore vein occurrence elements do not significantly affect the ratio. The findings of a detailed analysis of the Au:Ag ratio may be used for similar deposits and make it possible to classify ore bodies by their extent and mineralization concentration. Figures 2; tables 1; references 2.

On Value of Gold Nuggets

927D0229H Moscow RAZVEDKA I OKHRANA NEDR in Russian No 2, Feb 92 pp 29-30

[Article by N.V. Petrovskaya (deceased), B.G. Bychok, Institute of Ore Deposit Geology, Petrography, Mineralogy, and Geochemistry and Mineral Resources Institute; UDC 549.283]

[Abstract] The increasingly stringent requirements imposed on handling and managing the natural geological formations prompted a reevaluation of the issue of gold nuggets mined in the country. The origins of the term "nugget" and nugget characteristics are discussed and gold nuggets are divided into several categories according to their weight; the factors which determine the gold nugget cost in the world market are outlined and the regions of the world where the incidence of gold nuggets is significant are mentioned. The genesis of gold nuggets is discussed and it is speculated that they are endogenic in origin. The importance of sampling and examining gold nuggets for solving many applied geological tasks is stressed, especially for Russia where many gold placer deposits rich in nuggets are being explored. The poor state of gold nugget handling, certification, and storage is noted and five principal steps are suggested for improving the situation, particularly instituting a system of incentives for enterprises which promote complete nugget preservation and storage, supplying enterprises with a set of relevant manuals, setting up a centralized commission charged with gold nugget classification, grading, and pricing, advertising nuggets for sale abroad, and withholding especially valuable nuggets from commercial sales and preserving them for scientific study. References 1.

Rare and Scattered Elements in Surface Waters

927D0229I Moscow RAZVEDKA I OKHRANA NEDR in Russian No 2, Feb 92 pp 33-35

[Article by V.A. Vyushin, All-Union Institute of Geophysical Surveying; UDC 556.535:8:546.65]

[Abstract] The possibility of examining the concentration distribution of rare and scattered elements in surface waters for estimating their mean concentrations in water, using it as surveying criteria of ore deposits, determining the natural water contamination with heavy metals, and measuring the natural concentration levels of heavy metals as well as other applied tasks and solving the problems of background monitoring is discussed and data on the rare and scattered element distribution in surface waters of certain regions of European Russia are considered. The results of water analyses from selected water points in Kareliya, the lower Pripyat and Dnepr, and Podolsk highlands are summarized for F, Au, Cs, Sc, Co, and Sb. High or "hurricane" Sb, Cs, Sc, Co, and Au concentrations make it possible to expect the presence of a certain superposed component which characterizes the metallogenic or man-made features of the water catchment area. The mean concentrations of F, Au, Cs, Sc, Co, and Sb and the water mineralization levels are summarized and three water mineralization categories are identified. The dependence of the water mineralization on the mean element concentration is noted for all elements under study and it is noted that the presence of both actively migrating elements and weak migrants depends on the mineralization level; the high ore element concentration is attributed to the regional metallogenic specialization. The importance of the findings for environmental monitoring, especially at the start of a long observation period, is stressed. Tables 2; references 2.

Final Dressing of Off-Grade Rare-Metal, Quartz and Dump Mica Products in a Pneumatic Separator

927D0220K Moscow TSVETNYYE METALLY in Russian No 7, Jul 92 pp 72-75

[Article by G. V. Zadorozhnyy, S. N. Karnaukhov, and V. I. Maksimov, Kola Affiliate of the All-Union Research and Design Institute for Mechanical Processing of Minerals; UDC 622.778:621.318.3]

[Abstract] Results of research on dressing off-grade rare-metal, quartz and dump mica products in a pneumatic separator are presented. The pneumatic method was investigated as a way to process the non-conductive fraction of electric separation of coarse loparite concentrate, in which 10-12% of the ore is typically lost. As a result of the research,

the following processes were developed: dressing of fine-grain, off-grade loparite-bearing products which makes it possible to obtain a commercial loparite concentrate at a concentrating efficiency of 41.5%; dressing of dump vermiculite products which makes it possible to obtain a concentrate with 95% vermiculite content at a concentrating efficiency of 38.9%; and a process for obtaining commercial quartz grit and dust.

Possibilities of Photometric Separation of Pyrite-Bearing Barite Ores

927D0220J Moscow TSVETNYYE METALLY in Russian No 7, Jul 92 pp 70-72

[Article by V. I. Yershov, A. K. Voytenko, N. I. Zaytseva, and I. V. Shibina, small scientific-technical enterprise "Ekho"; UDC 622.7:535.24]

[Abstract] Possibilities of using the method of photometric separation in technology for dressing of barite ore having a high pyrite content are examined. The method permits dressing and conditioning of barite ore according to the content of its main components in the stage of coarse crushing. This was seen to be advantageous from the standpoint of reducing the volume of ore before transporting and processing at the dressing mill. In addition, the method could create conditions for obtaining suitable gravity-separated barite concentrates. Test processing was done on a sample of barite ore containing 57.1% $BaSO_4$ and 2.6% Fe_2O_3 taken from a conveyor of a dressing mill. Data are given on the fraction composition and distribution of components according to degrees of crushing of the ore, results of photometric separation of barite ore, and comparative indicators of ore dressing. It was found that it is possible to reduce the amount of ore transported from the mine to the dressing mill by 15.2%, as well as to reduce its processing in the stages of crushing, jigging and flotation. These factors alone are said to provide economic justification for photometric separation of barite ores. In addition, it is possible to obtain concentrate of suitable condition.

Metallurgical Waste—Raw Materials for Refractory Production

927D0208F Moscow OGNEUPORY in Russian
No 2, Feb 92 pp 23-25

[Article by T. V. Chusovitina, I. I. Ovchinnikov, N. L. Sizova, Ye. N. Menshikova, L. B. Khoroshavin, S. N. Tabatchikova, T. M. Golovina, and L. S. Beklemisheva, Eastern Scientific Research Institute of Refractories; UDC 669.002.68:666.762]

[Abstract] Results were presented from a technical and economic assessment of using various types of metallurgical waste in the production of refractory materials. Magnesia-silicate slags from the Serov ferroalloy plant were used to produce periclase-spinellid-forsterite linings for the anode furnace of the Kyshtym electrolytic plant. These linings were comparable in durability to chromite-periclase linings. Forsterite-spinel heating furnace bottoms for the Chelyabinsk forging press and forsterite-spinellid teeming vessels for the Chelyabinsk metallurgical combine were made from high-carbon ferrochromium slag at the Magnesite plant. The furnace bottoms were 2-4 times more durable than those made with conventional raw materials, and the teeming vessels were as durable as periclase-graphite vessels. Use of these slags is calculated to save 2.1 million rubles per annum in raw materials costs and 157,000 rubles per year in savings from reduced environmental damage. Savings from transporting and storing these wastes is expected to be 96.5 thousand rubles annually. The formulas used to arrive at these figures are presented, and other examples of refractories produced using metallurgical wastes are discussed. Tables 1; references 5: Russian.

END OF FICHE

DATE FILMED

5 Nov 1992